NAL PROPOSAL #225

SCIENTIFIC SPOKESMAN:

K.W. Chen
Department of Physics
Michigan State University
East Lansing, Michigan 48823

FTS/Off-Net 517-372-1910 + 353-5180

Excited Muon, Lepton Pair Production, W Production, and Deep Inelastic Muon Scattering in High Energy Muon Interactions

K.W. Chen, D. Fox, A. Kotlewski, P.F. Kunz

Michigan State University

L.N. Hand, S. Loken, A. Russell

Cornell University

CSL/G-07

Excited Muon, Lepton Pair Production, W Production, and Deep Inelastic Muon Scattering in High Energy Muon Interactions

ABSTRACT

A muon experiment is proposed to utilize high energy muons at 200 GeV in order to search for: (a) the possible existence of the excited, charged or neutral heavy muon, (b) the production of lepton pairs, $\mu^-\mu^+$, (c) to extend our study of the properties of the deeply inelastic μp reactions, and (d) for W-production or B^o-production via deep-inelastic muon scattering. The experimental apparatus consists of a muon spectrometer currently in use at the National Accelerator Laboratory to test scale invariance (Experiment #26), and a fine-grained total absorption calorimeter. The mass of excited or heavy leptons or W meson explored with this apparatus is up to 10 GeV. Final states of the produced particle are examined in sufficient detail with the calorimeter. We exploit the sharp cut-off in transverse momentum of daughter particles decaying from massive objects produced. Initially the experiment can be arranged to run parasitically with Experiment #98. A total of 10^{13} muons is requested, corresponding to 2×10^{18} protons incident of the Neutrino Laboratory target. A muon beam with μ/p of 5×10^{-6} is required.

TABLE OF CONTENTS

VIII. Appendices (continued)

FIGURE CAPTIONS

Figure 1. Proposed Layout

2. Side View of Apparatus

3. Apparent Scaling Breakdown Simulated by QED Modification

4. a) Ratio of Experimental WAB Cross Section to Theoretical Cross Section (QED)

   b) Limits on Searches of $\mu^* \rightarrow \mu + \gamma$ State

5. Calculated Trident Production Cross Section

6. Details of μ Trident Test of Fermi-Dirac Statistics (Muon)

7. Total Cross Section for Photo-production of Heavy Lepton Pairs

8. Search for M^+, M^- Using Hadronic Decay Modes

9. Differential Cross Section for Deep Inelastic Muon Scattering

10. Acceptance of this Apparatus for μp Deep Inelastic Scattering

11. μp Integrated Event Distribution in E-26 and this Proposal

12. B^0 Production Cross Section as a Function of Muon Energy

13. Calorimeter Performance Tests by Runge

14. Transverse Momentum Spectrum of e, π, or μ in Massive Object Decays

15. Photos of Experiment #26 Spectrometer

16. Photos of Experiment #26 Spectrometer

A_1. Pulse Height Digitizing Circuits

A_2. Pulse Height Digitizing Circuits

A_3. E-26 Spectrometer Details

A_4. Typical μp Deep Inelastic Event in E-26

A_5. Proposed Apparatus in Muon Area

I. INTRODUCTION

The proposed experiment, using high energy muons in the energy range up to 200 GeV, will permit us to: (1) search for an excited muon through a reach on $\mu+Z \rightarrow \mu^*+Z$, ($\mu^* \rightarrow \mu+\gamma$) up to a μ^* mass of $\tilde{-}$ 10 GeV^2/c^2 at a 400 GeV operation; (2) measure the cross section for the trident interaction $\mu+Z \rightarrow \mu\mu\mu+Z$; (3) extend the measurement of deep inelastic scattering $\mu+Z \rightarrow \mu$ + anything in the region $q^2 \geq 100\ GeV^2/c^2$; (4) search for a neutral or charged heavy lepton through a reaction $\mu+Z \rightarrow \bar{M}^0+Z$ or $\mu+Z \rightarrow M^+ + M^- + \mu+Z$, both the leptonic and hadronic decay modes will be considered, and (5) search for a W meson in a deep inelastic reaction $\mu+Z \rightarrow \mu+Z+W^{\dagger}$.

It is a fortunate aspect of high energy muon physics that these experiments can be accomplished in the relatively simple apparatus, without compromising any of them. The apparatus, which will be described in sufficient detail later, consists of a modular arrangement of liquid scintillator-lead plate counters and spark chambers which form a fine-grained ionization calorimeter and the same iron spectrometer currently in use by our group to check scale invariance (E-26). A sketch of the combined apparatus is shown in Fig. 1 and Fig. 2.

The principal aim of all of these experiments is to search in completely unexplored regions for fundamental structure in electromagnetic, weak and strong interactions.

The following is a short discussion on the open physics question we pose. A detailed discussion will follow.

1) For the pure electromagnetic interactions high energy muons open the possibility of studying pure leptonic processes

NAL MUON PROPOSAL

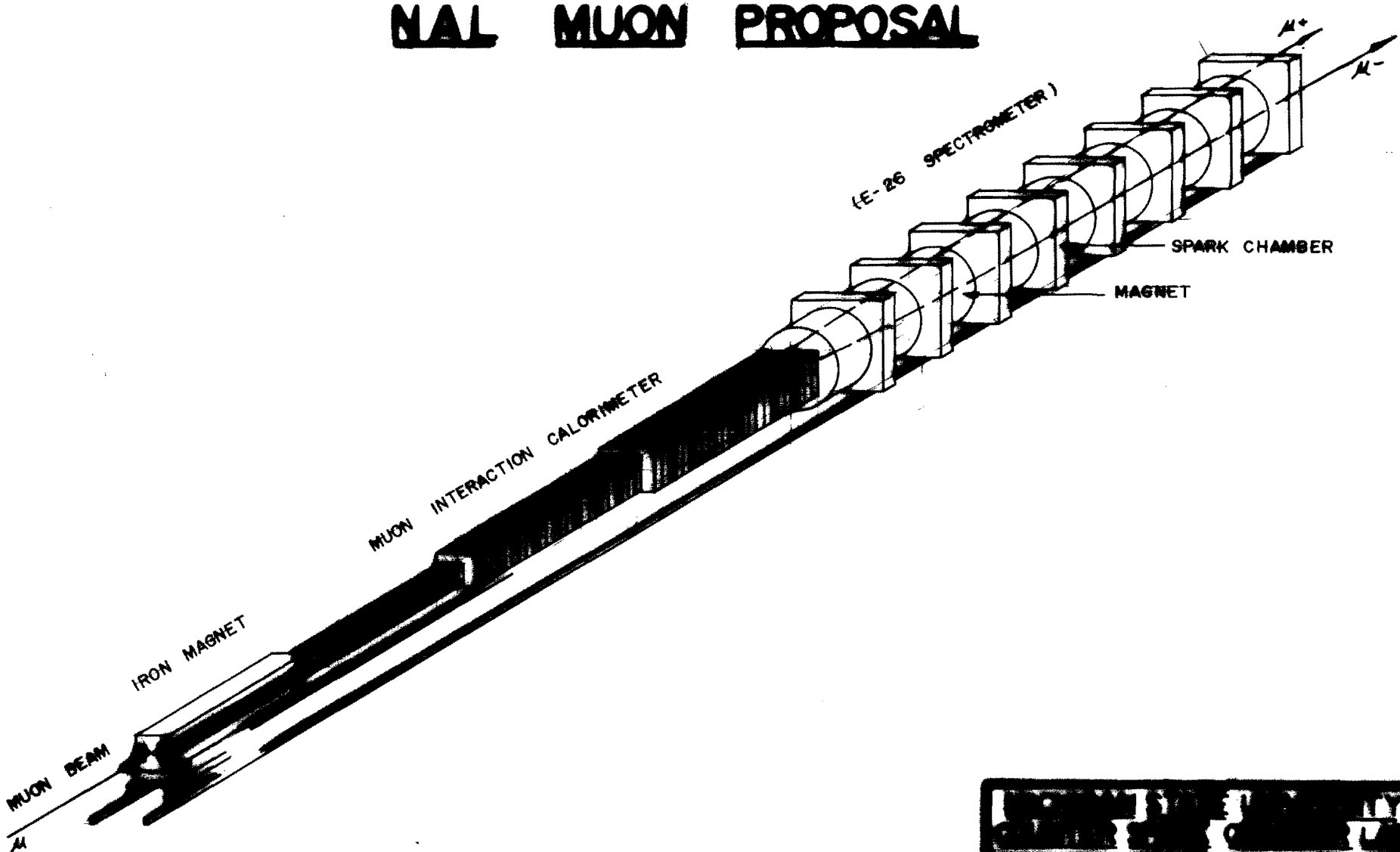

FIGURE 1

NAL MUON PROPOSAL

Scale: 3/32" = 1'-0" | Date: 3-30-73

NAL MUON PROPOSAL

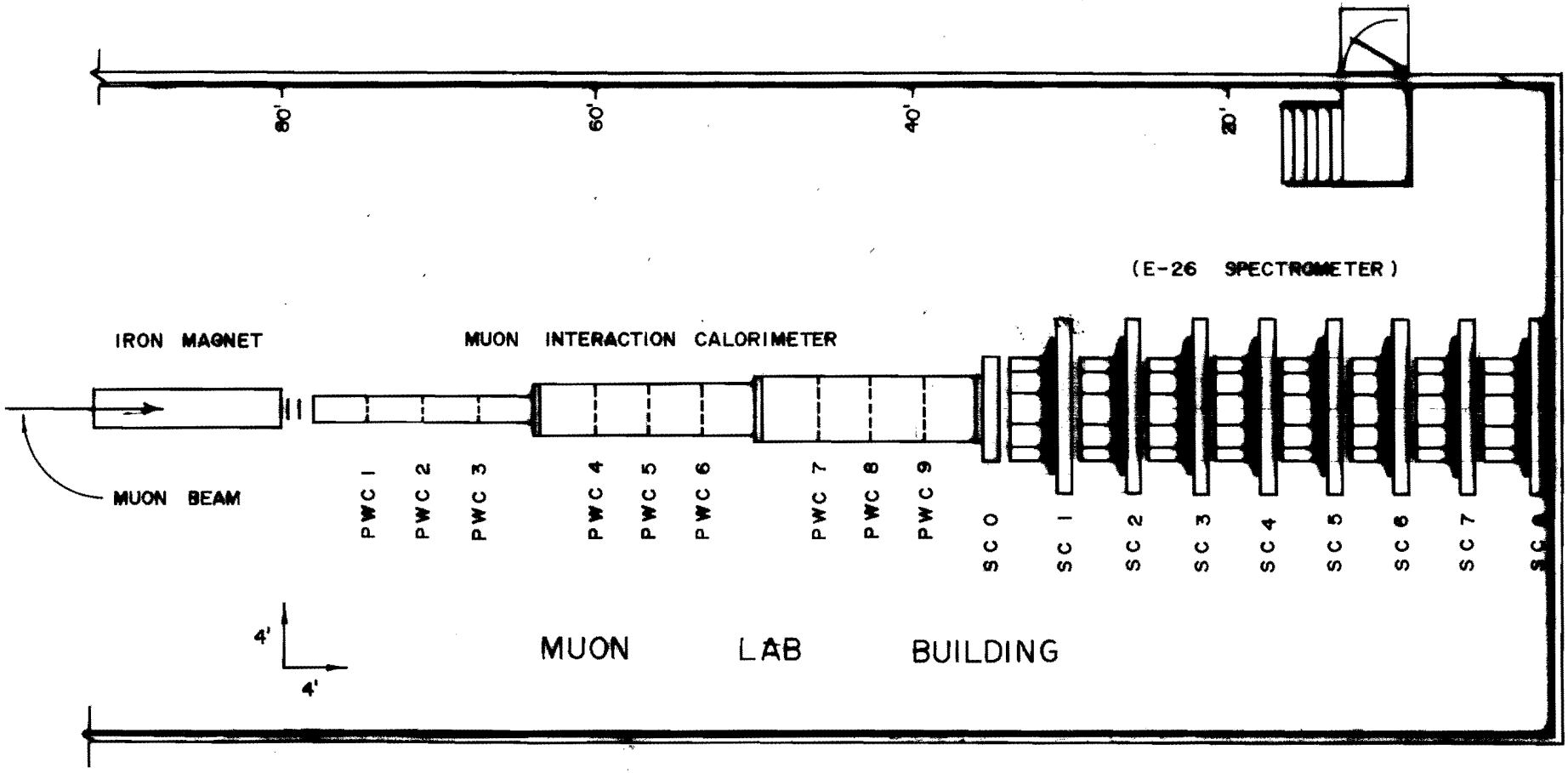

FIGURE 2

MICHIGAN STATE UNIVERSITY
COUNTER SPARK CHAMBER LAB

NAL MUON PROPOSAL

Scale: As Shown | Date: 3-30-73

Drawn by: | Approved by: | Drawing No.

such as trident production which investigates the muon propagator. This is also the only reaction to probe the muon-muon interactions. In addition, the possible existence of an excited muon, μ^*, has been suggested some time ago.[1] A search of this particle by looking at the decay mode $\mu^* \rightarrow \mu+\gamma$ has not yet been proposed.

2) The recently introduced spontaneously broken gauge theories of weak interactions avoids the high energy divergence of the Fermi theory, by introducing neutral currents or heavy leptons. Without heavy leptons, one must have neutral currents. In certain classes of theories proposed to date, neutral heavy leptons are introduced to cancel divergent diagrams involving exchange of a neutrino. The neutral leptons can be produced and detected via the reactions $\mu+Z \rightarrow \bar{M}^0 + X$; $\bar{M}^0 \rightarrow \mu^+ + \mu^-+\nu$. The charged heavy leptons can be produced and observed in the process $\mu+Z \rightarrow M^+ + M^- +\mu+Z$; M^+ and M^- decays into leptonic or hadronic states.

3) For the strong interactions, high energy muon allow us to extend the results on deeply inelastic scattering obtained in Experiment #26 to higher momentum transfers and thus to probe deeper into hadronic structure. We propose to study the regions in which q^2 exceeds 100 GeV^2/c^2.

4) There is also the possibility that the large energy transfers (>100 GeV) in deep inelastic muon scattering (at low momentum transfers) may allow a search of the W boson by $\mu+Z \rightarrow \mu+W^++z$. This target-fragmentation process has the same powers of the weak and electromagnetic coupling constants as the process $\nu+Z \rightarrow \mu+Z+W$, a familiar reaction in high energy neutrino search of the W.

In addition Lee and Wick proposed the existence of a hypothetical mass electromagnetic boson which would be produced in the reaction[11]

$$\mu + Z \rightarrow \mu + Z + B^{O}$$
$$\hookrightarrow \begin{cases} \text{leptons} \\ \text{and hadrons} \end{cases}$$

It is our contention that, for these measurements at high muon energies, massive electronic-spark chamber detectors and massive target are most useful, and in most cases, the only method. It is possible to design a system that exhibits many of the favorable properties of counter-spark chamber detectors, i.e., (i) a very large quantity of target material of appropriate Z, (ii) operation in a triggered electronic mode with fast timing and both coincidence and anticoincidence requirements, (iii) relatively clear and direct distinction between muons, photons, and pions that either do or do not decay in flight, and (iv) good angular resolution and measurement of particle multiplicities. It is also possible to approach in that design the sensitivity of a bubble chamber to low energy particles by making the detector sufficiently fine-grained,so that a minimum of information is lost within it.

The ionization calorimeter that we propose to add to E-26 Muon spectrometer is invaluable. It is carefully designed to meet three specific requirements:

1) Serves in Part as a Massive Target. A massive enough target of high Z provides a sufficient rate in trident production $\mu \rightarrow \mu\mu\mu$. To the extent that it meets this requirement, it is also a satisfactory target and detector with which to search for $\bar{M}^{O}$,

M^+, M^- or W and decay products.

2) Background Suppression and Event Selection. It should be sensitive to low energy hadrons and electromagnetic showers to distinguish "noisy" events from "quiet" ones and to suppress the copious background of inelastic scattering in the search for dimuon events. To optimize this sensitivity, lead is chosen as the material of the calorimeter primarily because, per radiation length, there is about 2.8 times more ionization loss in iron than in lead. Information lost in an iron calorimeter is not lost in a lead calorimeter. For example, a muon interaction involving a momentum transfer of 0.3 GeV/c to a bound proton will probably free that proton from the nucleus. The proton lead then, has a range 1.5 times greater than 0.5 radiation length of the grain size of our calorimeter. In contrast, the range of a proton of the same momentum in iron is less than ½ of 0.5 radiation length.

3) Kinematic Checks. The calorimeter should provide adequate measurement of the virtual photon energy and of the momentum transfer from the incident muon to the outgoing muon over a wide range of momentum transfers. In this connection, the fine-grained nature of the calorimeter proposed here will show superior resolution than coarser grained calorimeters, especially in sampling the electromagnetic part of showers.

Momentum measurements using the muon spectrometer of NAL Experiment26:

The use of E-26 spectrometer allows a measurement of outgoing muon momentum and transverse momentum. The sharp cut-off in

transverse momentum, a distribution of the decayed products from a massive object produced, is a powerful technique used in this experiment. This distribution will help in i) mass determination, and ii) in background rejection. The property of this spectrometer is well known. We have reason to believe that a muon momentum resolution of ±10% or better can be achieved. Transverse momenta are measured to ±150 MeV/c.

We now turn to a detailed discussion of the proposed physics program.

II. DETAILED DISCUSSION OF PHYSICS PROGRAMS

A. Search for an Excited Muon Through $\mu+Z\rightarrow\mu^*+Z$ ($\mu^*\rightarrow\mu+\gamma$)

The quantum electrodynamics (QED) of electrons, muons, and photons has so far been found to be in agreement with various experiments. This agreement has usually been expressed in terms of a fictitious "radius" down to which the theory has been found to hold. In this language, an experimental deviation from the theory would reveal a "cutoff".

A much more natural theoretical way of describing a breakdown of QED (and a more likely way for such a breakdown to occur) is in terms of coupling of electrons and muons to other particles. This is consistent with the ideas of ordinary quantum field theory and is the only theoretically consistent way to describe a real breakdown. Continued experimental confirmation of the predictions of QED would be expressed in terms of upper limits to the coupling strengths and lower limits to the masses of hypothetical particles coupled to electrons, muons, and photons.

This point of view suggests a class of experiments which would search directly for such particles by looking for correlations in the mass spectrum of groups of final electrons and photons just as is done in strong-interaction physics. These experiments would be direct checks of QED.

The following are several outstanding possibilities suggested:

(i) The muon might be coupled to a heavy excited muon, μ', with a magnetic coupling of the form

$$\lambda \bar{\psi}_{\mu'} \sigma_{\mu\nu} \psi_{\mu} f_{\mu\nu} + \text{H.C.} \qquad (1)$$

Assuming a mass of the μ' in the GeV range, existing experiments are consistent with a coupling strength $\Lambda \sim \frac{e}{m_e}$ provided a reasonable cutoff is assumed and provided the decays $K^{\pm} \to e^{\pm} + \nu$ and $K^{0} \to e^{\pm} + \pi^{\pm} + \nu$ are moderately forbidden. Otherwise, we must have $m_{e'} \gtrsim 1100$ MeV. The interaction (1) is neither minimal nor renormalizable. It would presumably be the low-energy manifestation of a minimal, renormalizable interaction (necessarily involving other particles) which would provide an automatic cutoff.

A possible reaction to search for this heavy excited lepton at NAL would be by means of a Primakoff-like effect

$$\mu + Z \to \mu^* + Z; \quad \mu^* \to \mu + \gamma \qquad (2)$$

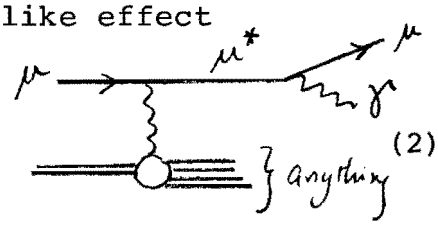

The simultaneous measurement of the muon and gamma energy and angle would allow a mass search.

(ii) The lepton (electron or muon) might be coupled to a boson, b, with an interaction of the form

$$g \bar{\psi}_{\ell} \Gamma_i i \psi_{\ell} b_i \qquad (3)$$

Again, assuming a mass m_b of the order of 1 GeV, existing experiments are consistent with $g^2 \lesssim e^2$, i.e., electromagnetic strength of coupling.

This particle would be directly produced in the process

$$\mu + Z \to \mu + Z + b \hookrightarrow \begin{cases} e^+ + e^- \\ \mu^+ + \mu^- \end{cases} (\sim 10^{-21} \text{ sec}) \qquad (4)$$

and would have to be observed directly as an $e^+ + e^-$ resonance, since strongly produced particles would make a missing-mass analysis difficult to interpret.

(iii) The muon might be coupled to an excited meson and a boson with an interaction

$$\bar{\psi}_{\mu'} \Gamma \psi_{\mu} b_i + \text{H.C.} \tag{5}$$

in which case there might be a conservation law. If so, the lighter of e' or b would be stable (except to weak decays). The production reaction would be

$$\mu + Z \rightarrow Z + \mu' + b \rightarrow \mu + \ell_1 + \ell_2 \tag{6}$$

where 1 is the lighter of b and μ'. The ℓ particle would now have to be found either by its charge or, if neutral, by its weak decay if any, and the (μ, M) mass spectrum measured to ensure that we were observing a deviation from QED. This case would obviously be the most difficult from which to extract information relevant to QED.[1] However, as will be discussed in II. C. and D., this case may well have pertinent information on the broken-gauge theories of weak interactions[2].

A careful search of μ^* should be carried for yet another reason. It has been conjectured that any breakdown of scaling could be a manifestation of modifications in QED at large momentum transfers[3]. The introduction of a Q^2 dependence in νW_2, could be caused in whole or in part to a QED modification in the photon propagator (i.e. one can express $\nu W = \left(1 + \frac{Q_2^2}{\Lambda}\right)^2 \cdot \nu W_2$. The effect of a μ^* to νW_2 is not as evident. However should it exist, one could entertain a diagram of the following kind in deep inelastic muon scattering

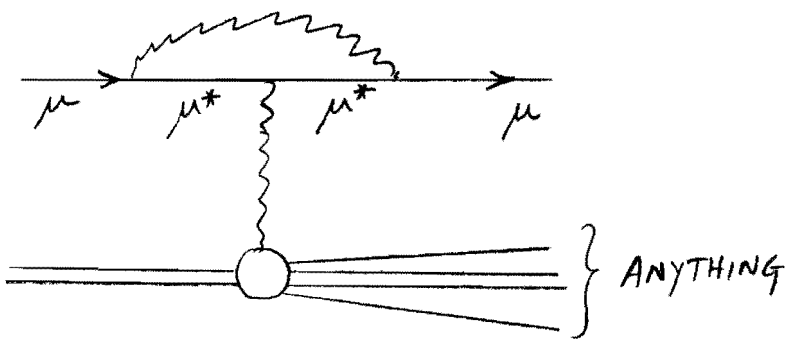

The net effect is similar to the conjecture of Nauenberg (see Fig. 3), that apparent scaling breakdown can be simulated by modification of QED. The bremsstrahlung cross section (commonly called the wide-angle bremsstrahlung) is estimated to be[4]

$$\frac{d\sigma}{dM_{\mu^*}} = 3 \times 10^{-33} \left(\frac{1}{M_{\mu^*}}\right)^4 \quad cm^2/GeV \tag{7}$$

where M is the mass of $\mu\gamma$ state. For a reasonable $\mu\gamma$ mass of 5 GeV, $\sigma = 10^{-35}$ cm^2. Experimentally, the μ^* signal competes with the single π^0 production

$$\mu + Z \rightarrow \mu + \pi^0 \hookrightarrow 2\gamma + \text{anything} \tag{8}$$

The experimental arrangement must resolve the 2 body events from 3 body events involving photon showers. The calorimeter we suggest could help in this endeavor. The contamination due to π^0 events is estimated to be 10% if a good angular resolution is assumed. However, it could well be that the sensitivity to μ^* in this experiment will be determined by our ability to distinguish single gamma events from multigamma events.

The latest experiment result [5] is shown in Fig. 4 a). The ratio of R, $= \frac{\sigma \text{ exp}}{\sigma \text{ th}}$ as a function of μ^* mass is shown. QED seem to be valid up to μ^* mass <1.2 GeV. The upper limit on the coupling

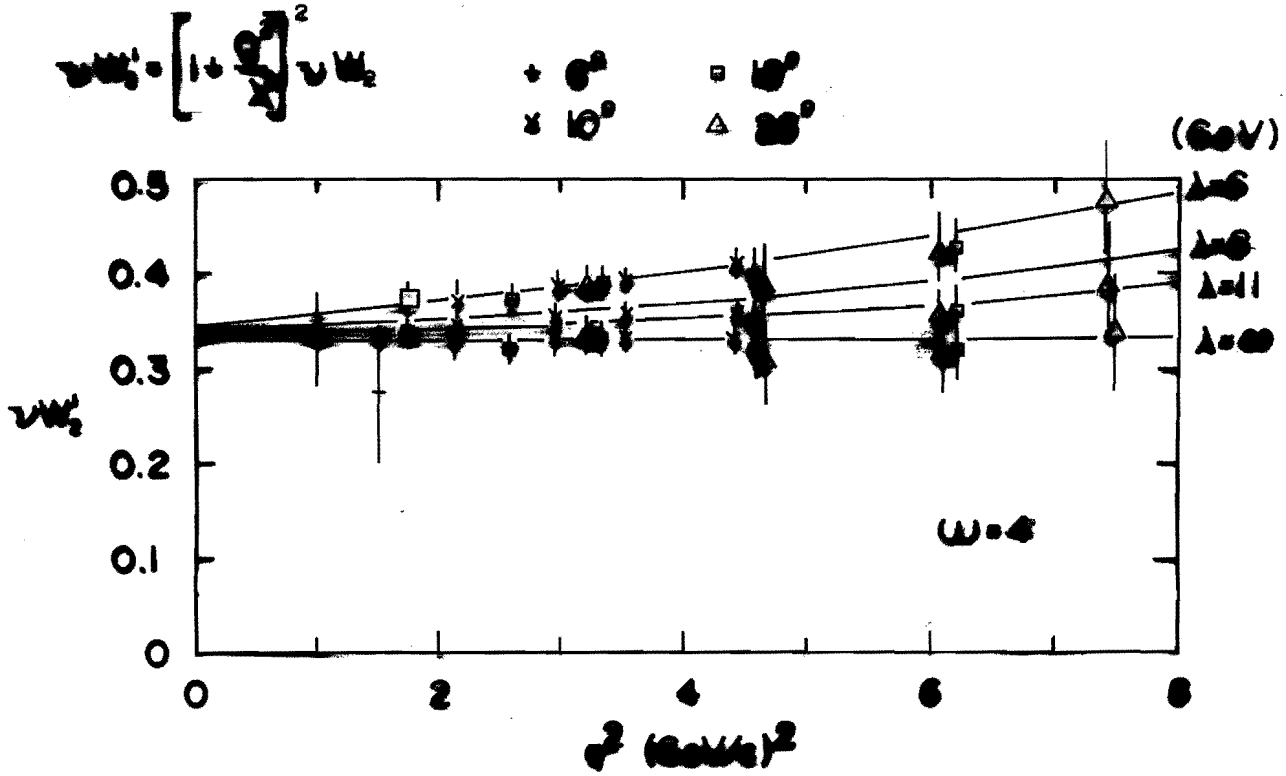

FIT OF νW TO A CUT OFF FUNCTION

FIGURE 3

RATIO OF MEASURED WAB CROSS SECTION TO QED PREDICTION

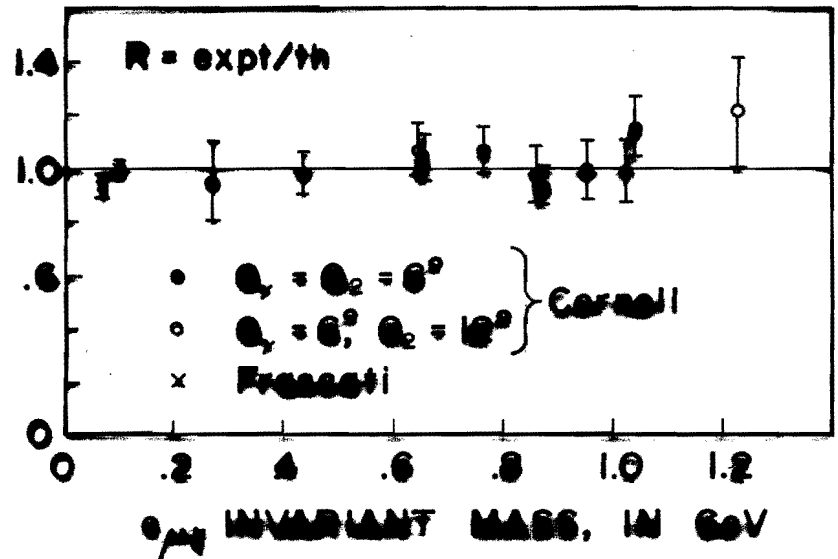

FIGURE 4a

FIGURE 4b

LIMITS ON SEARCHES OF $\mu^0 \rightarrow \mu + \gamma$ STATE

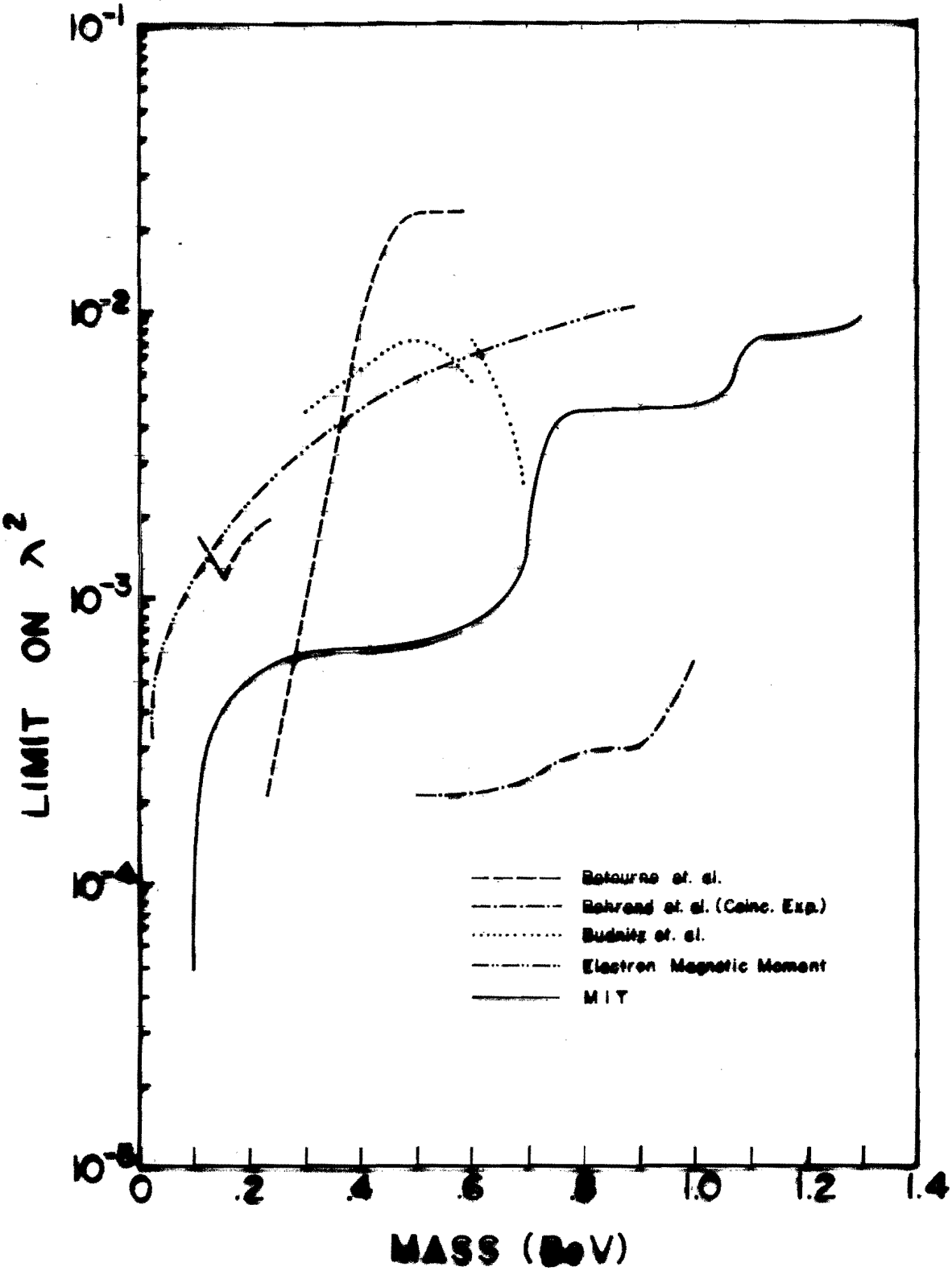

of the heavy electron λ ($\lambda \cdot e/m_e^*$) for the mass range 0.2 GeV < $m_{\mu^*(e^*)}$ < 1.32 GeV is shown in Fig. 4 b).

B. Study of Muon Statistics via Muon Pair Production by Muons

Muon pair production by muons is an important phase of the proposed experiment. A special appeal lies in the possibility of investigating the muon statistics. It is well known that states with two identical leptons must be antisymmetric with respect to the exchange of these leptons. At this time experimental verification of this statement in regards to muons has not yet been done at high energy. In particular a final state with two identical muons is of special interest. The reaction of the type $\mu^+ + Z \rightarrow \mu^+ + (\mu^- + \mu^+) + Z$ yielding a pair of leptons, is commonly called muon trident production. The trident reaction is interesting also from the point of view of quantum electrodynamics at small distances.

The complete differential trident cross section has been calculated for arbitrary helicities of incident and final particles.[6] Specific numerical calculations of these calculations are also available in the literature. Fig. 5 shows the calculated total cross section.

For a qualitative understanding of tridents, we can simply examine the Fegmann graphs relevant to tridents.

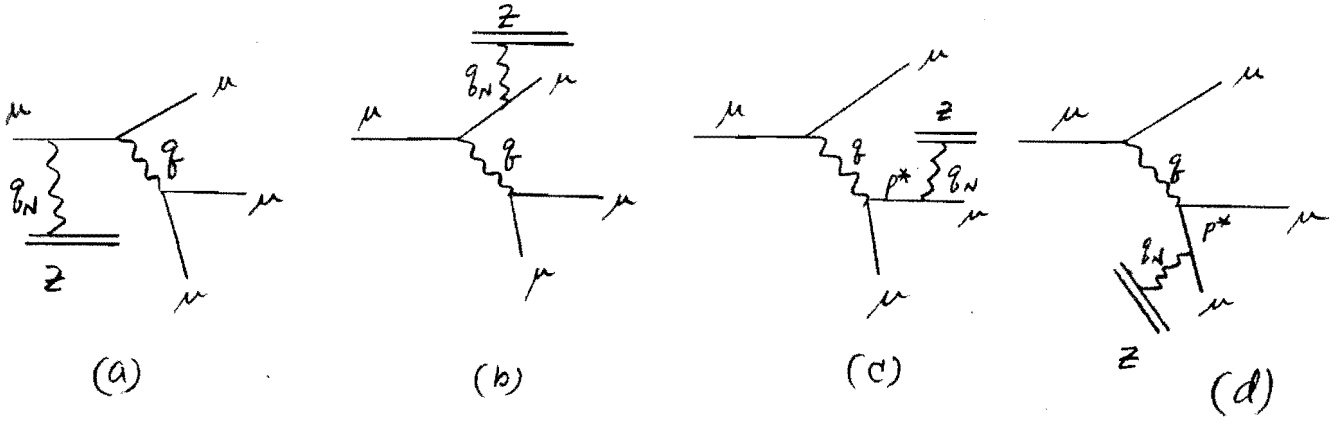

Then the square of each amplitude makes a contribution to the cross section as follows,

$$\frac{Z^2F^2\ (q_N^2)}{q_N^4}\ \frac{1}{q^4}\ \frac{1}{(p^{*2}+m_\mu^2)^2}. \qquad (9)$$

The trident differential cross section is largest in the regions of phase space where a term in any of the denominators of the eight possible matrix elements gets small. There are essentially four regions of phase space where the trident differential cross section is not vanishingly small:

(1) A lepton is collinear with the virtual photon q. In this case, $p^{*2}+m_\mu^2$ nearly vanishes for some diagram.

(2) A lepton of like charge is collinear with the incident particle. In this case, the spacelike virtual photon four-momentum squared is small (M_c and M_d).

(3) Two leptons of opposite charge are collinear in the final state. This means that the timelike virtual four-momentum squared is minimized (M_a and M_b) and is especially important for electron tridents.

(4) q_N, the nuclear recoil, is collinear with the incident lepton. This is the configuration in which q_N^2 takes on its minimum value when one of the final-state lepton momenta is varied while the other two lepton momenta remain fixed.

The energy distribution of the unlike muon (μ^- in the case of μ^+ beam and vice versa) is expected to be the most sensitive way to

examine the statistics of the muon for two reasons:

1) The opposite charge indicates the existence of a pair production process. (It could be also observed if a neutral lepton $\bar{M}^o$ were produced.)

2) Background processes are minimum.

At the highest energy for the unlike muon, the depression of cross section as a result of exclusion due to Fermi-Dirac statistics could be as high as 50%. Fig. 6 shows the possible sensitivity to this effect.

C. 1) Neutral Leptons, $\bar{M}^o$

The recent developments in unified gauge theories of weak and electromagnetic interactions have already been fruitful in focusing attention on the experimental question of the existence of leptonic and hadronic neutral currents.[7] Such currents arise because in some models a neutral heavy boson Z^o must exist in addition to charged intermediate bosons W. In other models, no neutral currents are needed, but additional heavy leptons are required (along, probably, with "charmed" heavy hadrons as well). It is probable that in any renormalizable theory of weak and electromagnetic interactions either neutral Z's or heavy leptons, or both, will be required.

It has been shown that most renormalizable theories will contain heavy leptons, and in any case it is of interest to understand the phenomenology of such particles. J. D. Bjorken and C. H. Lewellyn-Smith[2] summarized observable consequences of the existence of such heavy leptons in the context of these renormalizable gauge theories. The particles considered are M^+ and $\bar{M}^o$, $J=\frac{1}{2}$ fermions with

CALCULATED TRIDENT PRODUCTION CROSS-SECTION

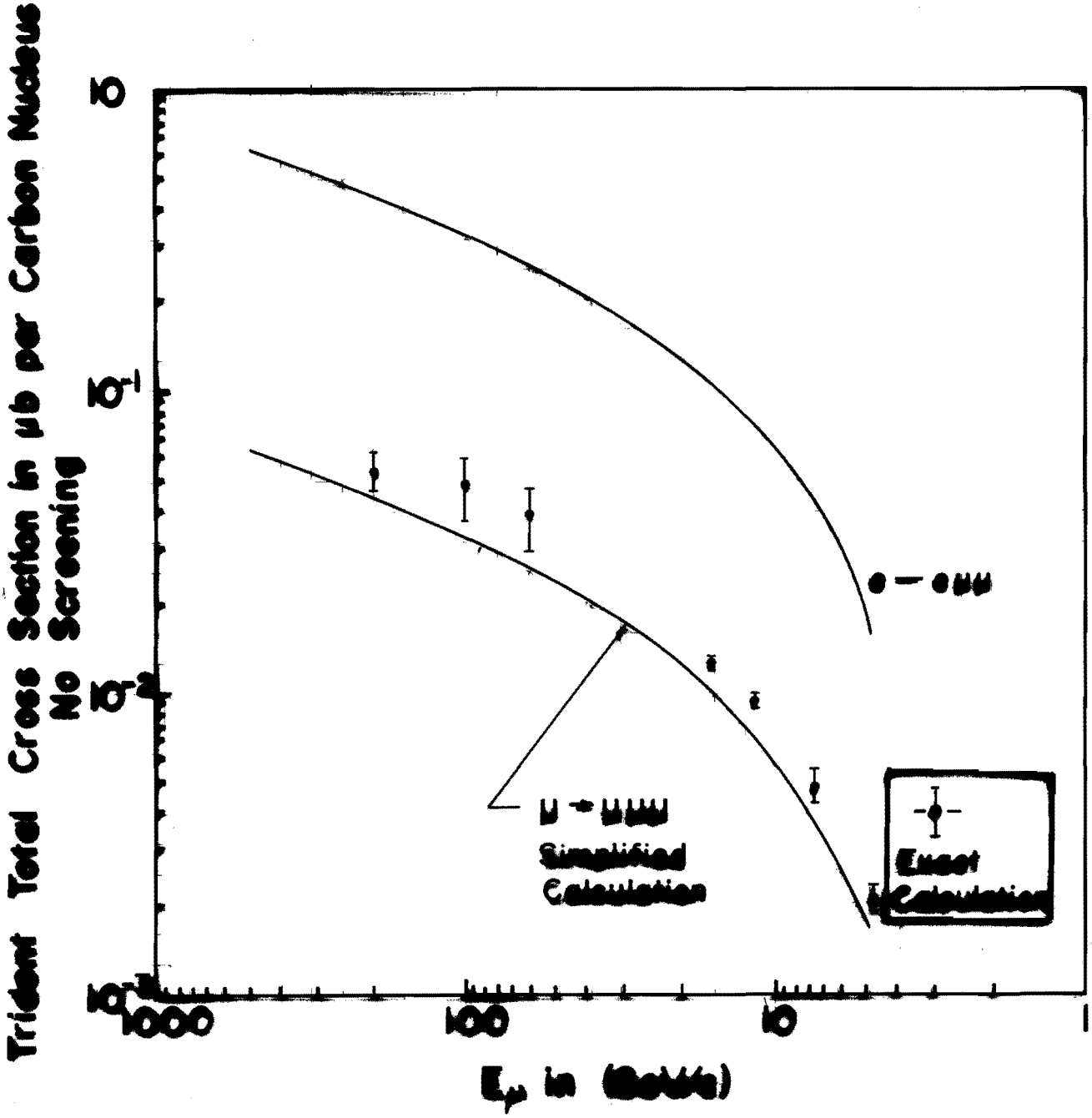

FIGURE 5 (REF. 6)

FIGURE 6 (Ref. 6)

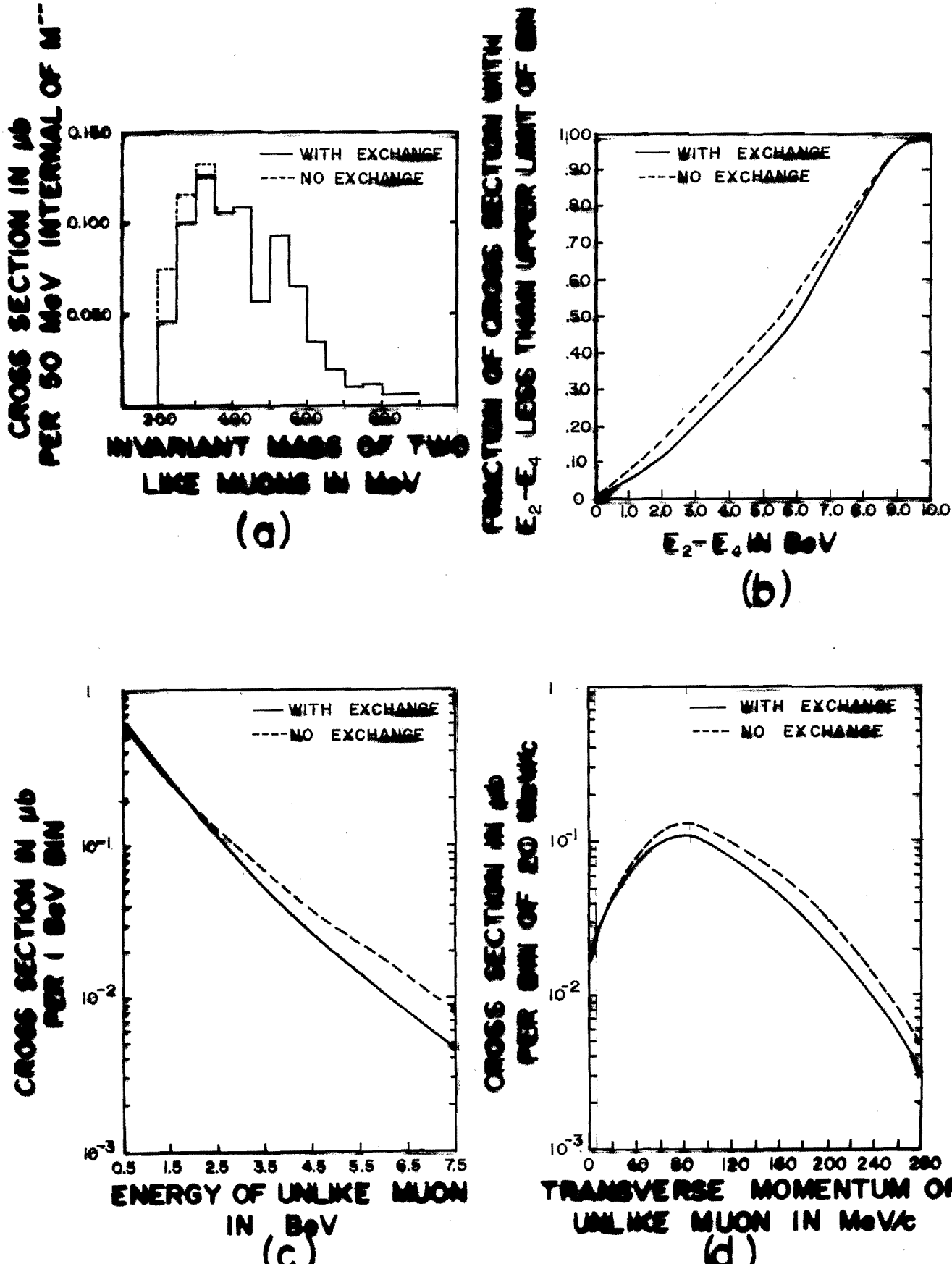

DETAILS OF μ TRIDENT PRODUCTION

the same lepton number assignment as the e^- (μ^-). Most of the theories contain $\bar{M}^o$ heavy lepton with (V+A) coupling. Other theories require $M^{\pm}$ which couple to leptons and neutrinos. Neutral heavy leptons have been searched mainly in weak interactions. The table shows limits on the mass of $\bar{M}^o$.

Table 1. Searches of Neutral Heavy Leptons.

Reaction Use	Limit on $\bar{M}^o$ Mass	Ref.
$K^+ \to e^+ + \bar{M}^o$ $K^+ \to \mu^+ + \bar{M}^o$	$\geq$ 0.5 GeV	
$e^+ + e^- \to \bar{M}^o + \nu$	0.9 GeV	Zichichi

The proposed search here employs the reaction

$$\mu + Z \to \bar{M}^o + x$$
$$\hookrightarrow \begin{cases} \mu^+ + \mu^- + \bar{\nu}_\mu & (\sim 25\%) \text{ (a)} \\ \mu^+ + e^- + \nu_e & (\sim 25\%) \text{ (b)} \\ \mu^+ + \text{hadrons} & (\sim 50\%) \text{ (c)} \end{cases}$$

The branching ratio of these decays are not known although, it has been speculated. The first decay mode (a) is the easiest to identify since two final state muons are observed. For decay modes, (b) and (c), electron and hadron identification are required.

The production cross section for $\bar{M}^o$ has been estimated using broken-gauge theory. For 100 GeV muons, it is estimated that

$$4 \times 10^{-37} \text{ cm}^2 \leq \sigma\ (\mu^+ + Z \to \bar{M}^o + \text{hadrons})$$
$$\leq 2.5 \times 10^{-35} \text{ cm}^2$$

provided that $M_{\bar{M}^o} < 4$ GeV. An experiment to search for $\bar{M}^o$ evidently must have an "effective luminosity" of 10^{35}.

C. 2) Charged Heavy Leptons, $M^{\pm}$

The charged heavy lepton can be muoproduction electromagnetically as

$$\mu+Z \rightarrow M^{+}+M^{-}+\mu+Z \qquad (10)$$

The Feynmann diagram of the reaction looks like

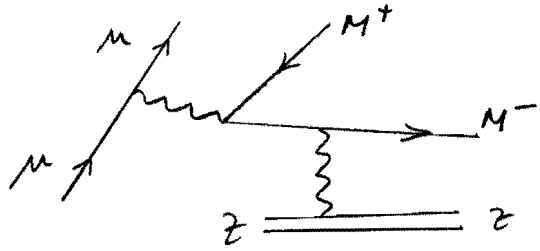

The production of $M^{\pm}$ via photoproduction (NAL #87) has been proposed already. The photoproduction cross section was evaluated by Kim and Tsai, shown in Fig. 7. To estimate the total cross section for muoproduction we estimate the lower bound by neglecting longitudinal virtual photon contribution. Averaging over k = 0 to 200 GeV, we estimate (Appendix A1)

$$10^{-37}\ \text{cm}^2 \leq \sigma(\mu+Z \rightarrow M^{+}+M^{-}+\mu+Z) \leq 10^{-36}\ \text{cm}^2 \qquad (11)$$

if $M_{M^{\pm}} \leq 3.0$ GeV.

D. Search of M^{+} and M^{-} Production by Hadronic Decay Modes

There is another way to detect the production of a $M^{\pm}$ with the reaction discussed in II. C. 2). The technique is used by NAL Experiment #1. The idea is based on the direct measurement of the recoiling M^{+} and M^{-} total energy and the event rate for the processes

$$\mu+Z \rightarrow \mu'+Z+M^{+}+M^{-} \quad \begin{cases} \rightarrow \text{hadrons} \\ \rightarrow \text{hadrons} \end{cases}$$

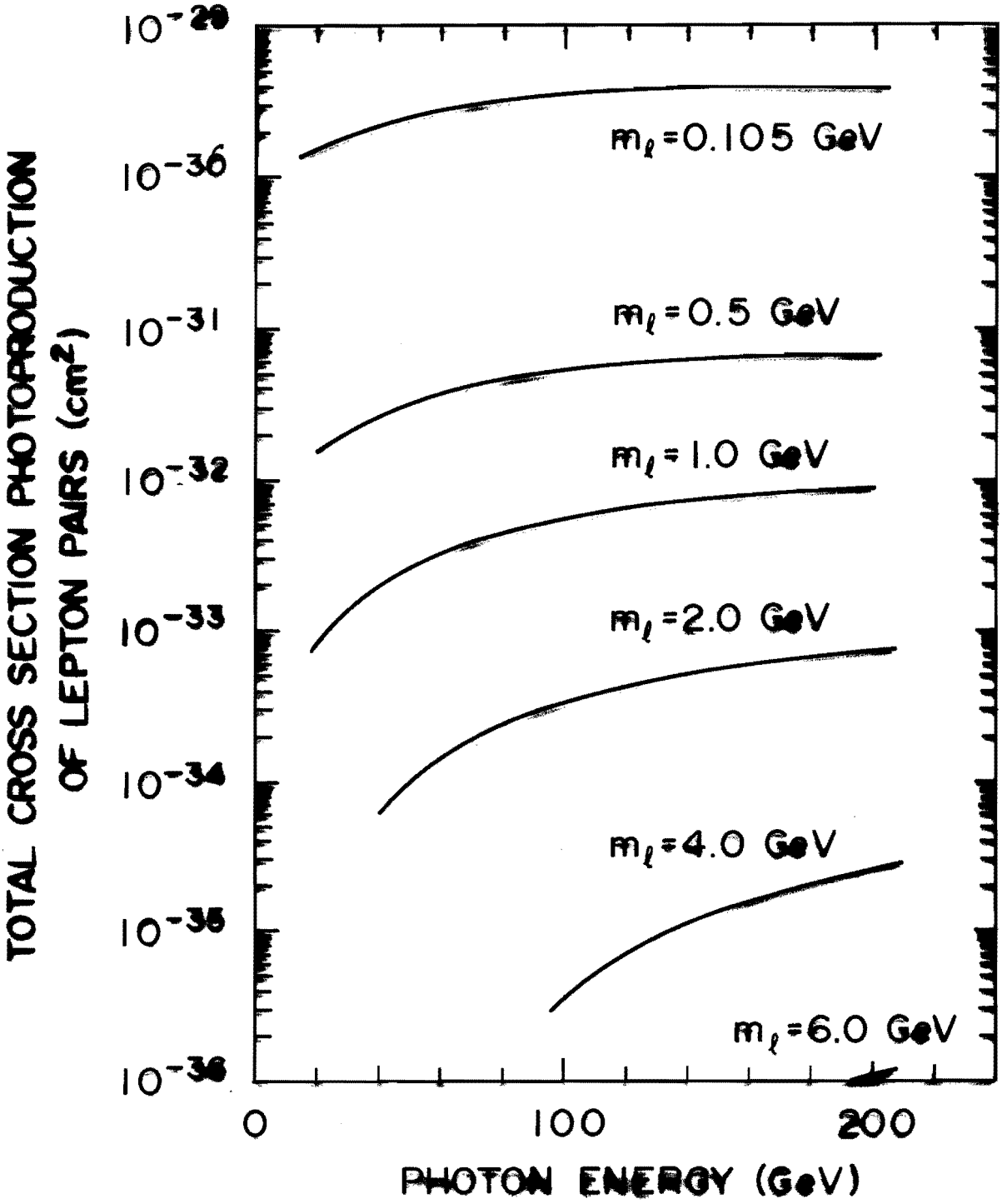

FIGURE 7 (Ref. 8)

This measurement, when combined with the M^+, M^- search via the leptonic decay mode discussed before, makes the overall search for the M^+ and M^- meson independent of any assumptions concerning the leptonic to hadronic branching ratio.

The basic ideas of the method are summarized as follows:

1. The measurement of the total hadronic energy from the M^+ (M^-) decay, plus the total μ^+ energy gives the virtual photon energy.

2. The characteristic kinematic features of M^+, M^- product are that the virtual photon energy is essentially all transferred to the M^+, M^- system and that the scattered muon receives a very small momentum transfer. Thus there will be a clustering of events coming from this process on the (q^2-ν) plot as shown in Fig.8.

3. The background inelastic events are expected to be smoothly distributed over the (q^2-ν) plot in the area where the M production events cluster. Thus an enhancement is searched in a predetermined region of the (q^2-ν) plot.

4. The E_μ dependence and absolute cross section for the production of events in the M enhancement region are calculable from theoretical estimates. Comparison of the data with these calculations gives a consistency check and allows a mass determination.

The magnitude of the background for $M^\pm$ production coming from the inelastic μ interactions can be estimated. We use the less controvertial diffraction model but also note that identical

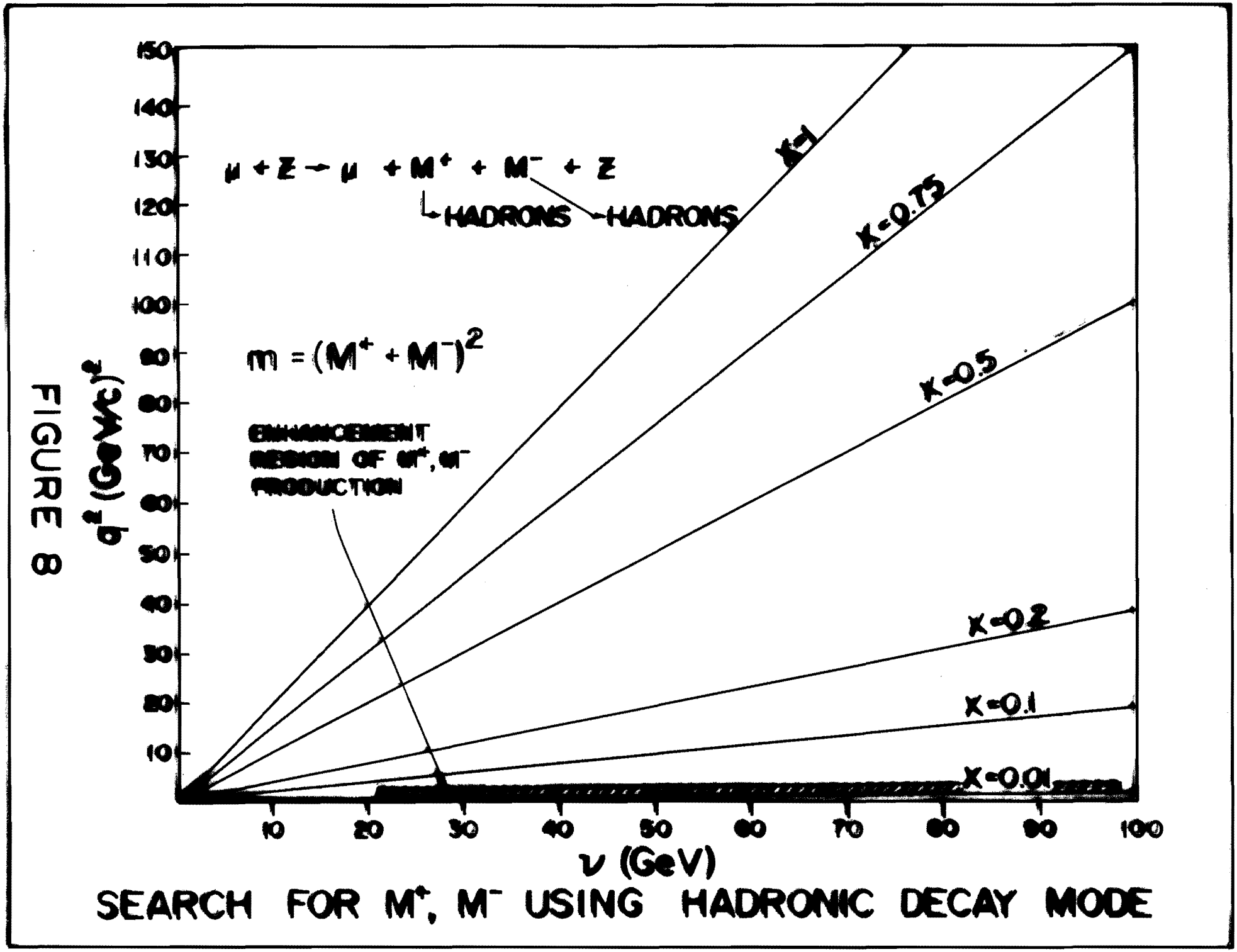

FIGURE 8

SEARCH FOR M^+, M^- USING HADRONIC DECAY MODE

conclusions would be obtained if the parton model is used. At any incident virtual photon energy the M^+, M^- production events are characterized by

$$y(=\frac{\nu}{E}) > 0.9$$

For $\nu(E_\mu - E_\mu')$ of 200 GeV, the M events will be produced with

$$x = q^2/2_M\nu \lesssim 2 \times 10^{-3}$$

The inelastic differential cross section for μ scattering on Pb (assuming equal (μ,n) and (μ,p) cross sections) is

$$\frac{d^2\sigma}{dxdy} = \frac{4\pi\alpha^2}{2m_p E} F_2(x,y) \frac{1}{x^2y^2}\left[(1-y)+ \frac{y^2}{2} \frac{1}{1+R(x,y)}\right] \qquad (12)$$

Our estimated cross section integrated over the (x,y) interval where M pair occurs is

$\sigma \lesssim 5 \times 10^{-36}$ cm^2 at 200 GeV for a M^+, M^- mass of 10 GeV.

In contrast the μ p deep inelastic scattering cross section in the same interval will be (at 200 GeV)

$$\iint \frac{d^2\sigma}{dxdy}\, dxdy \simeq 2 \times 10^{-37} \text{ cm}^2. \qquad (13)$$

Thus the M events will appear above background. For appreciable hadronic branching fractions (say 50%), the M production is by far the most efficient method of transferring a large amount of energy to the hadronic system for low momentum transfer. These events are quasicoherent events but with an enormous energy release to the hadrons.

We believe, therefore, that the M^+, M^- production events for which the M subsequently decays into hadrons can be uniquely separated from background through the observation of a bump in the cross section for inelastic scattering in a predetermined region of the (q^2-ν) plot. If the rate of M decay into hadrons were known, the absolute cross section for the M production would give the mass directly.

In the apparatus proposed to be discussed in the next section, both leptonic and hadronic decay modes of the W are detected with high efficiency. If the M were discovered, the leptonic to hadronic branching fraction would be obtained. In addition for any division of the branching fraction into hadrons and leptons, a M signal would be observable if the M^+, M^- mass were below the mass of $\sim$ 11 GeV. Thus by using all decay modes the mass range of the M can be extended and the question of the existence of the M below this mass can be answered without ambiguity.

E. Further Measurement of Deep Inelastic Muon Scattering

Currently Experiment #26 [9] plans to study muon inelastic scattering up to $q^2 \leq 100$ GeV$^2/c^2$. We first summarize E-26, then proceed to discuss the proposed experiment.

The experiment is designed to test scaling with the following parameters.

Table II. Parameters of E-26

Incident Muon Flux	0.3×10^{12}	
Target Thickness	24"	
Events Expected	$q^2 > 95$ GeV$^2/c^2$	100
	$q^2 > 80$ GeV$^2/c^2$	600
	$q^2 > 35$ GeV$^2/c^2$	10,000
Muon Energy	60, 100, 160 GeV	

Experiment #26 incorporates a method to test scaling by a physical scaling of apparatus. The principal advantage of the idea is an elimination of systematic errors to test scaling accurately.

Without the outcome of E-26, it is difficult to project the interest of μ-p deep inelastic scattering at $q^2 > 100$ GeV$^2/c^2$. However, should scaling fail to break down in E-26, a serious study of scaling is obviously called for at higher q^2.

This part of the experiment has the following rate advantages over E-26.

DIFFERENTIAL CROSS SECTION FOR DEEP INELASTIC MUON SCATTERING KINEMATICS

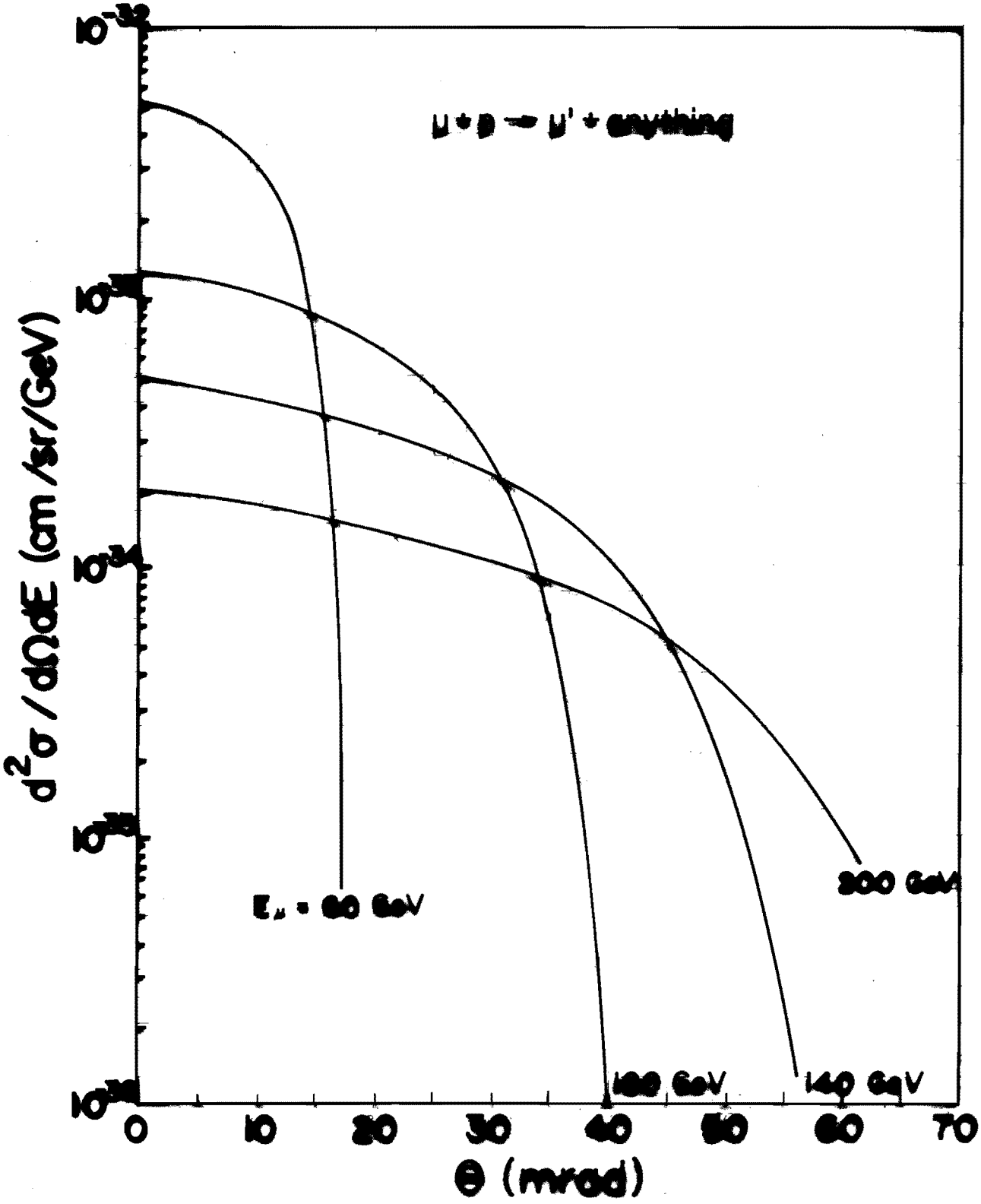

FIGURE 9

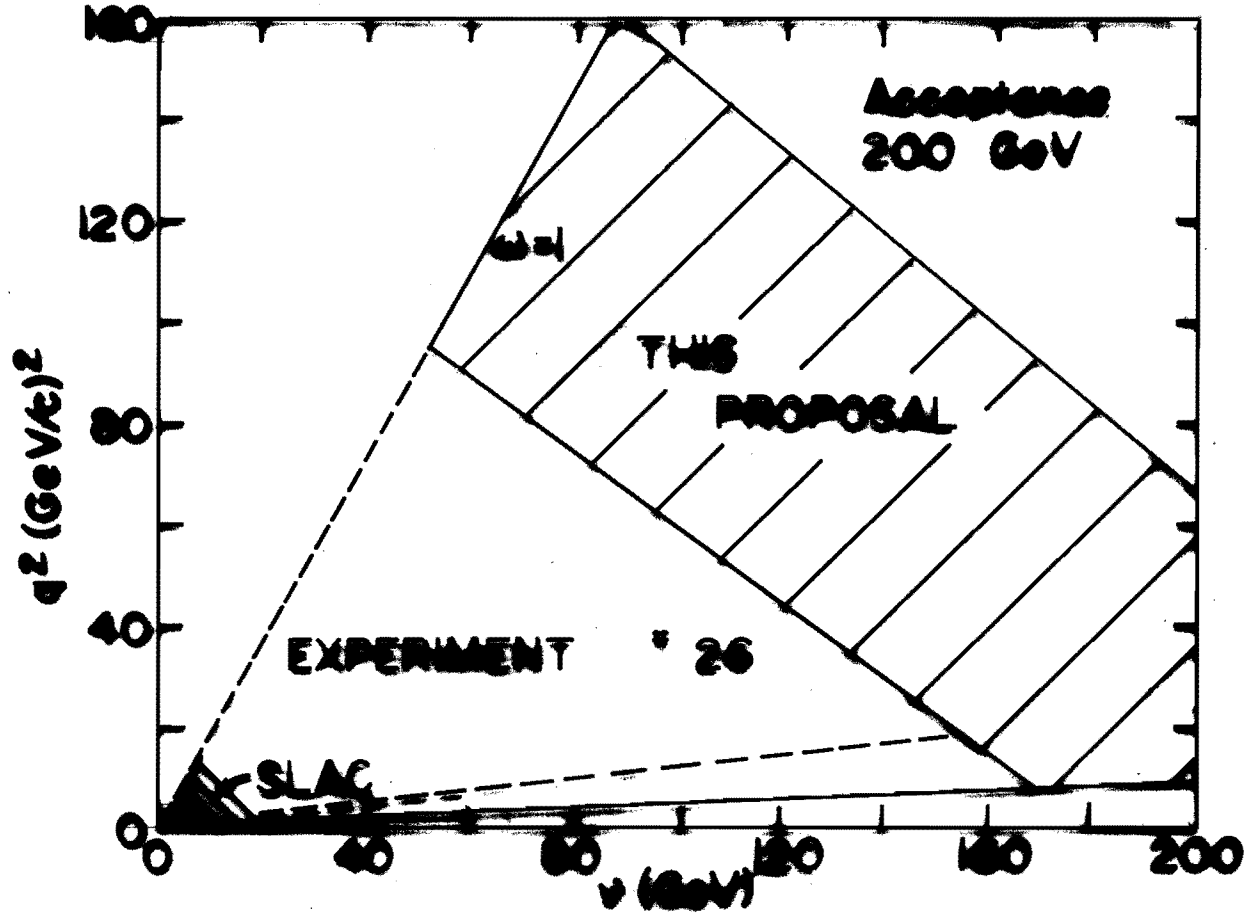

FIGURE 10

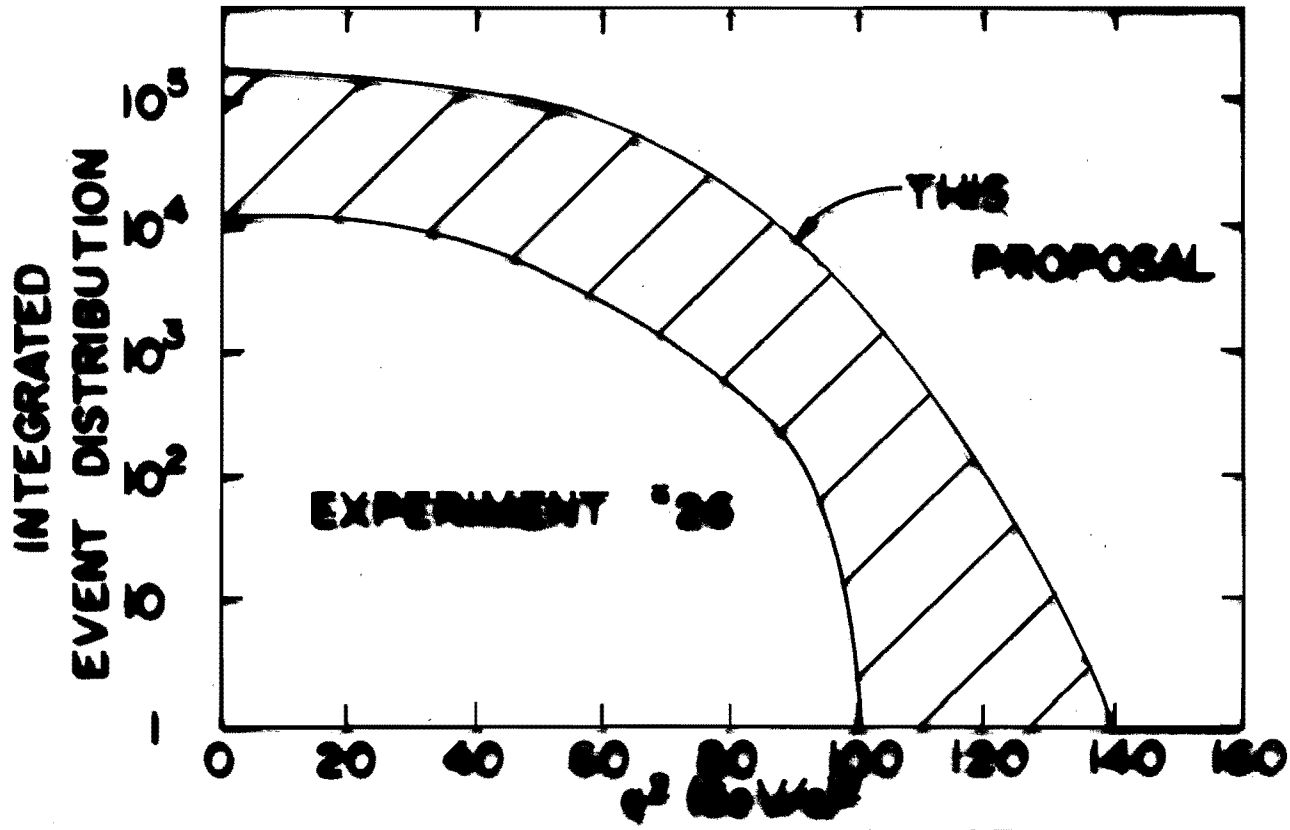

FIGURE 11

EVENT DISTRIBUTION FOR μp
DEEP INELASTIC SCATTERING

Beam Flux	$10^{12}/0.3 \times 10^{12}$	= 3.3
Target Thickness	256"/24"	= 12.0
Total Rate Increase Factor		40

A 40-fold increase in rate increases the region of q^2 by 2.2. Thus in principle it is feasible to explore the region up to $\sim$ 200 GeV^2/c^2. However, the acceptance of the spectrometer (limited by the aperture) will restrict the detection of high q^2 events. It is estimated that there should be $\geq$ 100 events in the region $q^2 \geq$ 150 GeV^2/c^2.

We show in Fig. 9 the differential cross section for deep inelastic μ p scattering , and in Fig. 10, the region of q^2 and ν expected. Folding into the acceptance, the integrated event distribution is shown in Fig. 11, comparing it with expected E-26 results.

F. Other Processes

1. W Production Process

W bosons may be produced by muon beams in the reactions $\mu+Z \rightarrow \nu+Z+W$ (projectile fragmentation) and $\mu+p \rightarrow \mu+n+W$ (target fragmentation). Using a model in which strong-interaction effects via phenomenological form factors are introduced, Fearing, Pratap and Smith[10] studied the target fragmentation process, concentrating on energies and W-boson masses appropriate to NAL. Total cross sections and angular and energy distributions for the W boson and the final muon are given and compared with those obtained in the projectile-fragmentation reaction. The calculation includes the possibility of an anomalous magnetic moment for the W boson. The

Feyman diagrams are of the following

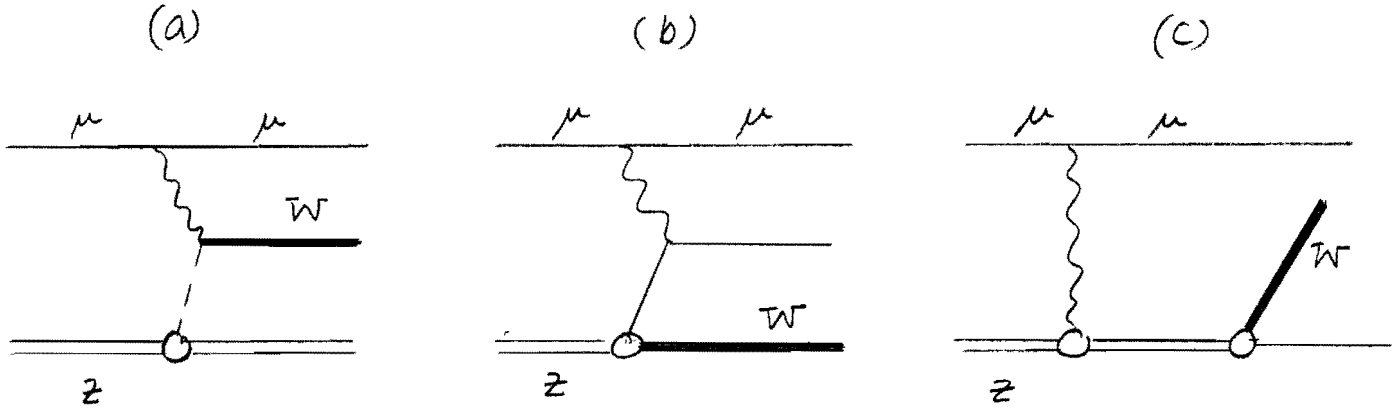

The interaction with the target is entirely of electromagnetic nature; thus the only form factors which must be considered are the usual electromagnetic form factors of the nucleon or nucleus.

There is, however, another W-boson production reaction possible with muon beams which has the same powers of the weak and electromagnetic coupling constants as the two above. This reaction, namely,

$$\mu^- + p \rightarrow \mu^- + n + W^+, \tag{15}$$

or the corresponding neutron target reaction

$$\mu^- + n \rightarrow \mu^- + p + W^-, \tag{16}$$

is essentially W production via deep-inelastic muon scattering. It differs from

$$\mu + Z \rightarrow \nu + Z + W \text{ and } \nu + Z \rightarrow \mu + Z + W \tag{17}$$

in that the W is produced at a hadronic vertex as a result of target fragmentation. Thus for a realistic calculation one must now include form-factor effects at the weak pnW vertex as well as at the electromagnetic vertices. Also, since the target nucleon changes its charge, there is no coherent reaction on a heavy nucleus as in reactions

$$\nu+Z \rightarrow \mu+Z+W \qquad (18)$$

The result of Fearing et. al. is summarized in Table IV.

TABLE IV.

Total cross sections 200 GeV incident muon energy for the reaction $\mu+p \rightarrow \mu+n+W$ for two W-boson masses, $k^W = 0, \pm 1$, and for the three assumptions about form factors described in the text. For comparison we have included some results in the W-W approximation and results for the reaction $\mu+n \rightarrow \mu+p+W$.

	$\mu + p \rightarrow \mu + n + W$			
M_W	$k^W=0$	$k^W=0$ W-W approx.	$k^W=+1$	$k^W=-1$
		No Form Factors		
5 GeV/c^2	4.51×10^{-35}	4.67×10^{-35}	4.53×10^{-35}	4.56×10^{-35}
10 GeV/c^2	1.63×10^{-35}	1.70×10^{-35}	1.63×10^{-35}	1.63×10^{-35}
		Constant Time-like Form Factors		
5 GeV/c^2	1.21×10^{-36}	4.69×10^{-36}	1.21×10^{-36}	1.21×10^{-36}
10 GeV/c^2	3.09×10^{-35}	3.09×10^{-35}	3.09×10^{-35}	3.13×10^{-35}
		Dipole Time-like Form Factors		
5 GeV/c^2	2.55×10^{-39}	2.73×10^{-39}	1.02×10^{-38}	9.47×10^{-42}
10 GeV/c^2	6.89×10^{-41}	7.69×10^{-41}	2.76×10^{-40}	1.20×10^{-44}

The total cross sections are quite reasonable ($\lesssim 10^{-36}$ cm^2) and definitely feasible! Although it is unlikely that there is no form

factor or a constant form factor, the true value could be found between the dipole time-like form factor and the two mere optimistic choices.

One observes that the total cross section is nearly independent of W-mass at high energy. If the total cross section is of the order of 10^{-37} cm^2 with an efficiency for detection ¼, we could estimate a rate of a few hundred W's in the course of this experiment. The kinematics of W detection, after it is produced, is quite simple. We shall not attempt to discuss it here.

2. Lee-Wick Massive Electromagnetic Boson

It has been suggested[11] that a hypothetical massive electromagnetic boson, B^o, might exist in the deep inelastic reaction

$$\mu + Z \rightarrow \mu + Z + B^o \quad \rightarrow \begin{cases} \text{leptons} \\ \text{hadrons} \end{cases} \tag{19}$$

Feymann diagrams for B^o are shown below

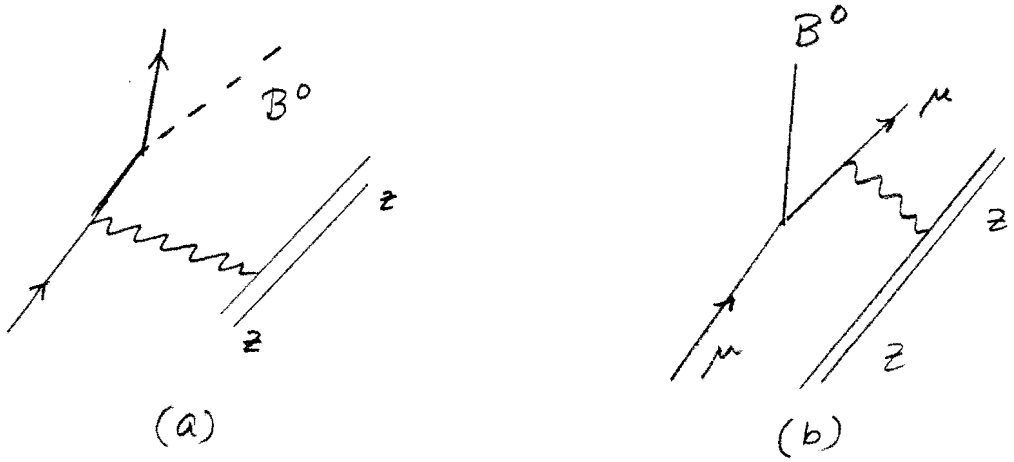

The total cross section for the B^o production was calculated by R. Linsker.[12] Several (Z,Z') cases have been studied, corresponding to elastic scattering off protons and neutrons (with and without

an exclusion principle), coherent scattering off spin-0 nuclei, and inelastic scattering off protons (in which case Z' denotes a nucleon resonance or hadronic system in the continuum). Detailed structure-function data are used to improve the accuracy of the inelastic scattering calculation. At a beam energy of 200-300 GeV, the cross section exceeds 10^{-36} cm^2, provided the B^0 mass is not much greater than 10 GeV.

The results of Linsker's calculations are shown in Fig. 12 for M_{B^0} = 7 GeV/c^2 and 10 GeV/c^2 respectively. Other detailed values are available for different masses and targets. We note again that the production section per nucleon is given in the neighborhood of 10^{-35} cm^2 to 10^{-37} cm^2, a cross section measurable in this experiment.

B^0 PRODUCTION CROSS SECTION AS A FUNCTION OF MUON ENERGY

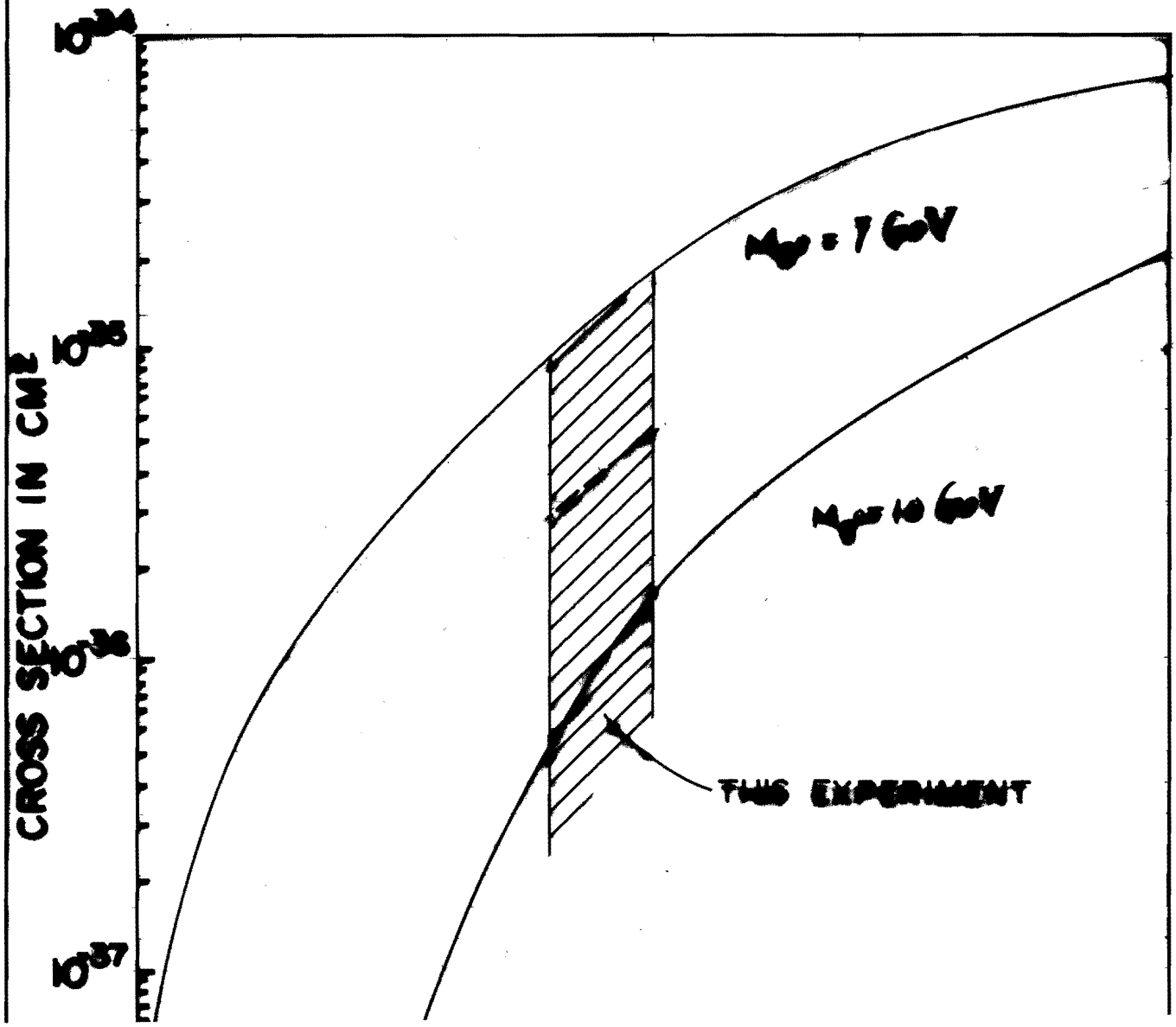

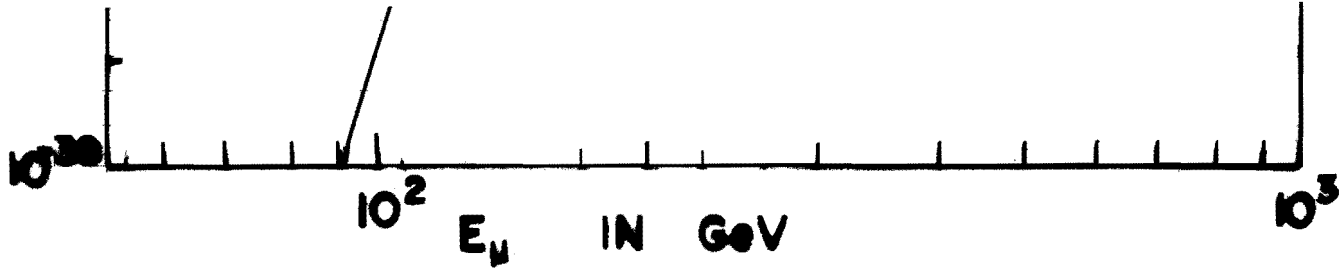

FIGURE 12 (Ref. 12)

III. THE EXPERIMENTAL ARRANGEMENT

A. The NAL Muon Beam

If the NAL beam components were to remain unchanged, improvements in proton beam emittance, extraction stability, and alignment of various elements in the neutrino target hall would raise the average yield of NAL muon beam intensity to 3×10^{-8}.

At the present moment, the following minor beam improvements are also contemplated:

TABLE V

	Expected gain in intensity
Put 3Q84's in Encl. 100	x 1.8
Encl. 101 aperture: 2 x 3 in → 4 x 4 in	x 3.0
Encl. 104 aperture: 2 x 4 in → 4 x 4 in	x 1.5
Improved vertical trimming and alignment downstream of absorber in Encl. 103	x 1.2
Total	x 10

The existing "target load", which momentum-selects hadrons for the "dichromatic" neutrino beam, produces a beam spot which is poorly matched to the muon beam aperture. A simple triplet lens with aspect ratio near unity would increase the muon intensity by a factor of at least seven. Depending on the needs of the neutrino program, such a lens could be folded into a dichromatic arrangement, or used in a horn bypass.

Increase of muon energies to 200 GeV will at least increase the muon yield by a factor of two. A FoDo channel in the decay tunnel gives a factor increase from 10 to 100.

It is entirely possible that a yield of 5×10^{-6} 200 GeV muons/400 GeV proton, can be achieved with a small financial commitment by NAL, although it will be necessary for the laboratory to further develop the muon beam. With this yield, the required 10^{13} muons correspond to 2×10^{18} protons. 2×10^{13} protons/6 sec on target, the integrated muon flux required by this experiment could be produced in 5×10^{4} pulses. For comparison, the proposed muon beam at CERN has a μ/p of 10^{-4}.[13]

B. Iron Deflection Magnet

It is proposed here that the muon beam is initially shared with E-98. A small iron deflection magnet is required to deflect the beam. The proposed arrangement of beam sharing is shown in the actual floor drawing, Fig. 3. In order to steer the muon beam properly, the magnet has a $\int B.dl$ equal to E-98 cyclotron magnet in operation. The muon beam is 8" x 10" at the exit of E-98 apparatus. A 12 ft. iron magnet with rectangular cross section, 16" x 16", is sufficient for this purpose.

The muon beam is shifted by 12.2" from the center beam line. The iron deflection magnet steers the muon beam horizontally by 14 mrad (following E-98 apparatus). After this magnet the parallel muon beam enters the muon-interaction apparatus. The iron are magnet grade steel slabs, 6" in thickness. The physical dimension is 2' x 2' x 12', weighing a total of 17 tons. This weight is approximately the same as one of the magnets now used in E-26 at NAL. This magnet costs $\leq$ \$10,000 to fabricate, following our own experiences in constructing 8 toroidal iron spectrometer magnets for Experiment #26.

The iron magnet also serves in part as a target for reactions described in sections II. B, C, E and F. The magnet is, however, not instrumented to detect photons or hadrons in the final state.

In the event that E-98 apparatus is inactive, the iron deflection magnet is turned off so that the muon beam traverses directly into the muon interaction apparatus to be described below.

C. Muon Interaction Ionization Calorimeter (MIC)

The muon interaction calorimeter offers the following experimental functions: (i) It is the target for the heavy and excited lepton search, for muon pair production experiments, and for the deep inelastic muon scattering in the region not yet covered by Experiment #26. (ii) It detects and measures the energy E_h of combined hadronic-electromagnetic showers produced in the reactions $\mu+Z \rightarrow \mu$ + (anything), and it measures part of the energy of the μ; the energy E of the muon initiating the reaction is check from the sum $E_h+E_{\mu'}$.

The design of the calorimeter (see Summary of Parameters, Appendix III) has been chosen to optimize its functions in the lepton pair production measurement because that is intrinsically the most difficult one. Pb is chosen as the material of the calorimeter. It is 35% more effective per ton than Fe in producing muon pairs and stopping power is 3/4 times that of Fe while its radiation length is about 1/3 that of Fe. Apart from requiring 1.35 times as many tons, the substructure of an Fe calorimeter is less favorable because per radiation length there is about 2.8 times more ionization energy dissipated in the Fe (as opposed to the scintillator) than in Pb.

The latter is an important feature in distinguishing electronically noisy events (photons, electrons, high energy mesons) from quiet ones (muons, low energy mesons). Specifically quiet events are those with two muons present in the calorimeter and, possibly, in the event of $\bar{M}^0$ or M^+, M^- production, a low energy ($\gtrsim$ 0.5 GeV) nucleon released in the calorimeter. Noisy events will in general contain only one muon and a hadron-electromagnetic shower. It is particularly necessary to discriminate against those noisy events which are only mildly noisy and which simulate the two muon property of quiet events through the decay in flight of an energetic π^+ meson. A single Pb plate thickness of 0.5 radiation length (plus aluminum cladding) corresponds approximately to the range of a 0.05 GeV proton; hence the calorimeter has the sensitivity to select a class of events that show two muons and either no or a very soft hadron shower. We estimate that the calorimeter will detect with high efficiency hadron showers with as little as (0.1 - 0.2) GeV energy content and that more than ~ 95 percent of the noisy events in which a π^+ decays in flight will in fact be identified as noisy.

A muon interaction in the iron deflection magnet target will give rise to one or more hadrons and an energetic muon incident on the ionization calorimeter. These are distinguished from useful muon interactions in the calorimeter by scintillation counters at the front of the calorimeter. In either case the hadron cascade will be completely absorbed before the event is considered useful.

It is useful to define the elasticity coefficient k of a muon interaction by $k = \nu/E_\mu$, where ν = virtual photon energy. Both k, E_μ and also the multiplicity may vary widely from event to event.

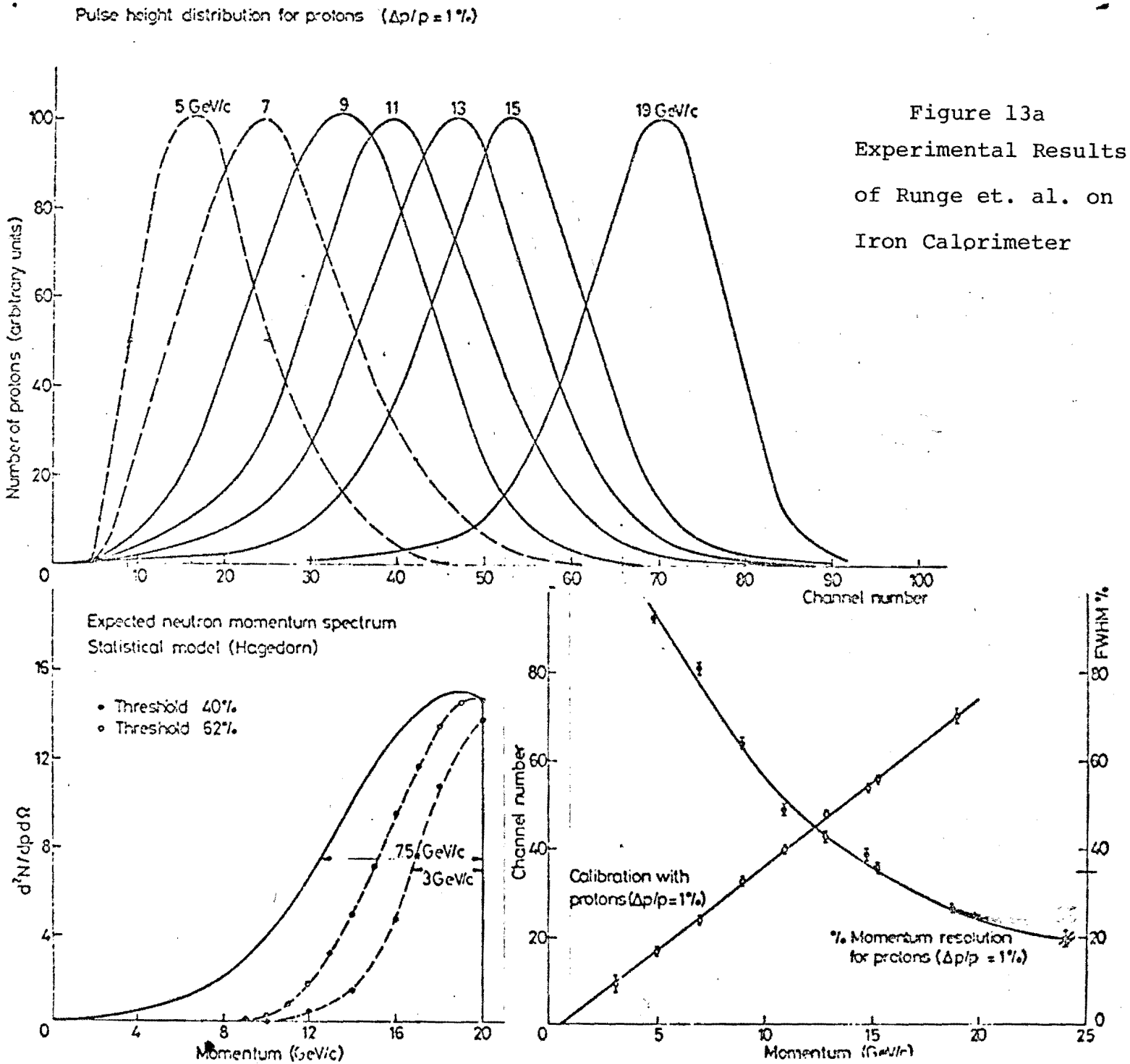

Figure 13a
Experimental Results
of Runge et. al. on
Iron Calorimeter

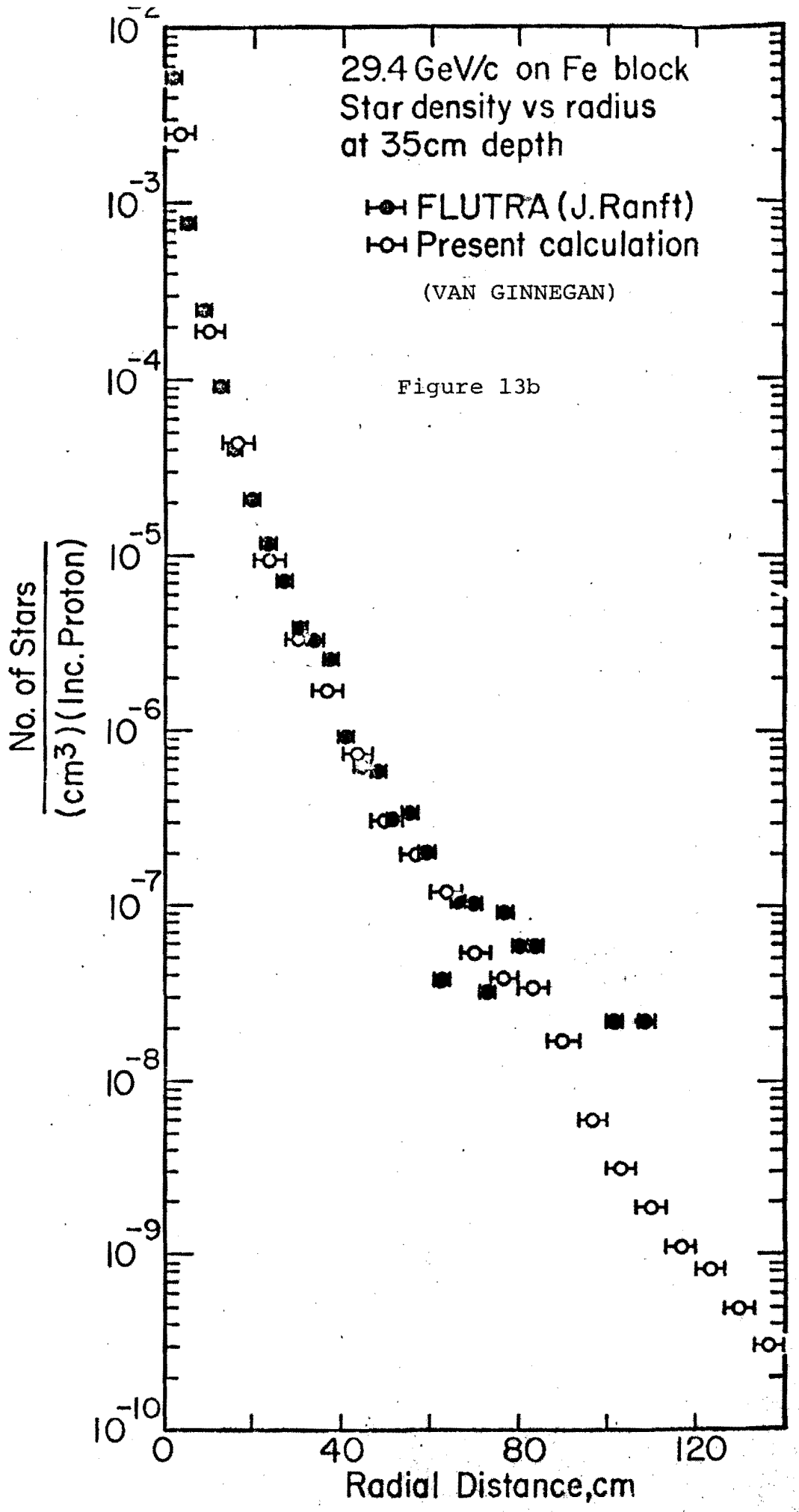
29.4 GeV/c on Fe block
Star density vs radius
at 35cm depth
FLUTRA (J.Ranft)
Present calculation
(VAN GINNEGAN)
No. of Stars / (cm³)(Inc. Proton)
Radial Distance,cm
0
40
80
120
10⁻²
10⁻³
10⁻⁴
10⁻⁵
10⁻⁶
10⁻⁷
10⁻⁸
10⁻⁹
10⁻¹⁰

Figure 13b

Nevertheless, it is likely that almost all events can be measured with $\Delta E_\mu/E_\mu \lesssim = 0.1$ over the entire region 190 GeV $\lesssim E_\mu \lesssim$ 210 GeV and for any value of k. This conclusion is indicated by the work of Runge,[14] who studied the properties of an iron plate calorimeter at CERN. The calorimeter consisted of 20 Fe plates 40 cm x 40 cm x 4 cm thick and 20 scintillator plates also 40 cm x 40 cm but of 1 cm thickness. The calorimeter was calibrated with protons in narrow momentum intervals of $\Delta p/p \sim 1\%$. Two methods were tried: (i) protons were forced to interact in an iron slab in front of the calorimeter or (ii) any proton hitting the calorimeter was accepted for pulse-height analysis; both methods gave identical results for linearity and resolution. Runge's results are shown in Fig. 13 which shows the pulse height distributions and momentum resolution of the calorimeter.

As an illustration of the use of Fig. 13 consider the interaction of a 20 GeV muon to yield a μ^- with k = 0.5 and a hadron cascade of 25 GeV. Assume for the present that E_μ can be measured with $\Delta E_\mu'/E_\mu' = \pm 0.13$ in the E-26 spectrometer, we obtain $\Delta E_h/E_h = \pm 0.12$.

This work is substantiated by similar work at the AGS, by experience in cosmic ray physics and by recent successful use of an ionization calorimeter in a neutron cross section experiment. It is consistent with detailed calculations by Ranft[15] and Van Ginnekan.[16]

IV. DISCUSSION OF EXPERIMENTAL TECHNIQUES

A. Muoproduction and Muon Radiation Lengths

When a muon is used for production of particles, the virtual photon process is significant compared with the real photon process if the target thickness is of the order $\tilde{<}$ 0.04 radiation lengths. This fact is well known among experts but is not familiar to others because the virtual photon process is proportional to α^4 whereas the real photon process is proportional to α^6.

The energy loss of a muon due to the bremsstrahlung is negligible compared with that due to the ionization when the energy is so low that its range is considerably less than one muon radiation length. However, when the muon energy is several hundred GeV or higher, its range becomes comparable to or greater than one muon radiation length. After a muon passes through a material of thickness comparable to one muon radiation length, its energy is greatly affected by the bremsstrahlung. We show that the apparatus proposed here does not suffer from these considerations. An approximate expression for the bremsstrahlung of a high energy muon is given by[8]

$$\left(\frac{d\sigma_b}{dk}\right)_{muon} = \frac{4\alpha r_0^2}{k}\left(\frac{m_e^2}{m_\mu^2}\right) Z^2 \left\{\left(\frac{4}{3} - \frac{4}{3}y + y^2\right) \ln\left[\frac{2E}{m_\mu}\frac{(1-y)}{y}\right] - \frac{1}{2}\right\}. \quad (20)$$

The muon unit radiation length x_μ can be written in terms of the usual electron radiation length x_o as

$$x_\mu/x_0 = \left(\frac{m_\mu^2}{m_e^2}\right) \frac{Z^2 \ln(183\ Z^{-1/3}) + Z\ln(1440\ Z^{-2/3})}{Z^2 \ln \frac{2E}{m_\mu}\frac{(1-y)}{y}} \quad (21)$$

which has a magnitude of slightly less than $(m_\mu/m_e)^2 \simeq 4 \times 10^4$.

In Table I we show the component thickness of the apparatus in muon radiation lengths.

Table VI.
Components of Apparatus in Radiation Lengths

Component	Material	Thickness (Meter)	Thickness in Radiation Length (for Muons)
Iron Deflection Magnet	Iron	3.7	0.0051
Calorimeter	Lead	4.8	0.0168
E-26 Spectrometer	Iron	6.5	0.0067
Total		14.95	0.0286

The proposed apparatus is optimized ($\lesssim$ 1 muon r.ℓ.) so that virtual photon contribution dominates the real bremsstrahlung.

B. Final State Muons and P_T Distribution

The broad program we envisage requires a clear understanding of trigger conditions in order to suppress copious background. To state it briefly, the experimental apparatus is designed to optimize signal rate (by the choice of symmetry), suppression of background by use of an ionization calorimeter, and by a selection of large transverse momenta particles. A detailed discussion of muon production is found in Appendix I.

1) Single Muon Detected

a) We study here deep inelastic muon scattering at high momentum transfers. The trigger for this experiment is the same

as E-26. The chief difference is the increase of a factor 12 in target thickness. This part of the experiment is triggered by the same electronic arrangement as E-26 now in operation.

2) Two Muon Detected

Here we measure $\bar{M}^o$ production or W^+ production via deep inelastic scattering.

a) $\bar{M}^o$ production. The reaction $\mu+Z \rightarrow \bar{M}^o + X$; $\bar{M}^o \rightarrow \mu^+ + \mu^- + \bar{\nu}_\mu$ can be observed in our apparatus. The mass of the lepton is reconstructed by measuring momenta of μ^+ and μ^-.

b) W^+ production. A feasible process of interest which could yield a final state with two muons is the W production via a target fragmentation process: $\mu+Z \rightarrow \mu'+W^++Z$ (23)

$W^+ \rightarrow \begin{cases} \mu\nu\nu \\ \pi\nu \\ \ell\nu \\ \text{hadrons} \end{cases}$

The experimental technique employed here is to observe the large transverse momentum, P_T, from the daughters of a massive object with mass m. There is a sharp cutoff at m/2. For forward particles, the resolution in projected transverse momentum in this equipment is ~ 120 MeV/c. The error is thus 10% at m = 2.4 GeV and improves with increasing m.

Hadronic decays of the W^+ or $\bar{M}^o$ will be separated by using the calorimeter and a technique discussed in Section II. D. The idea is to search for a clustering of hadronic decay events with large energy transfers in low q^2 region.

3) Three Muon Detected

a) Heavy lepton pair creation by muons.

FIGURE 14

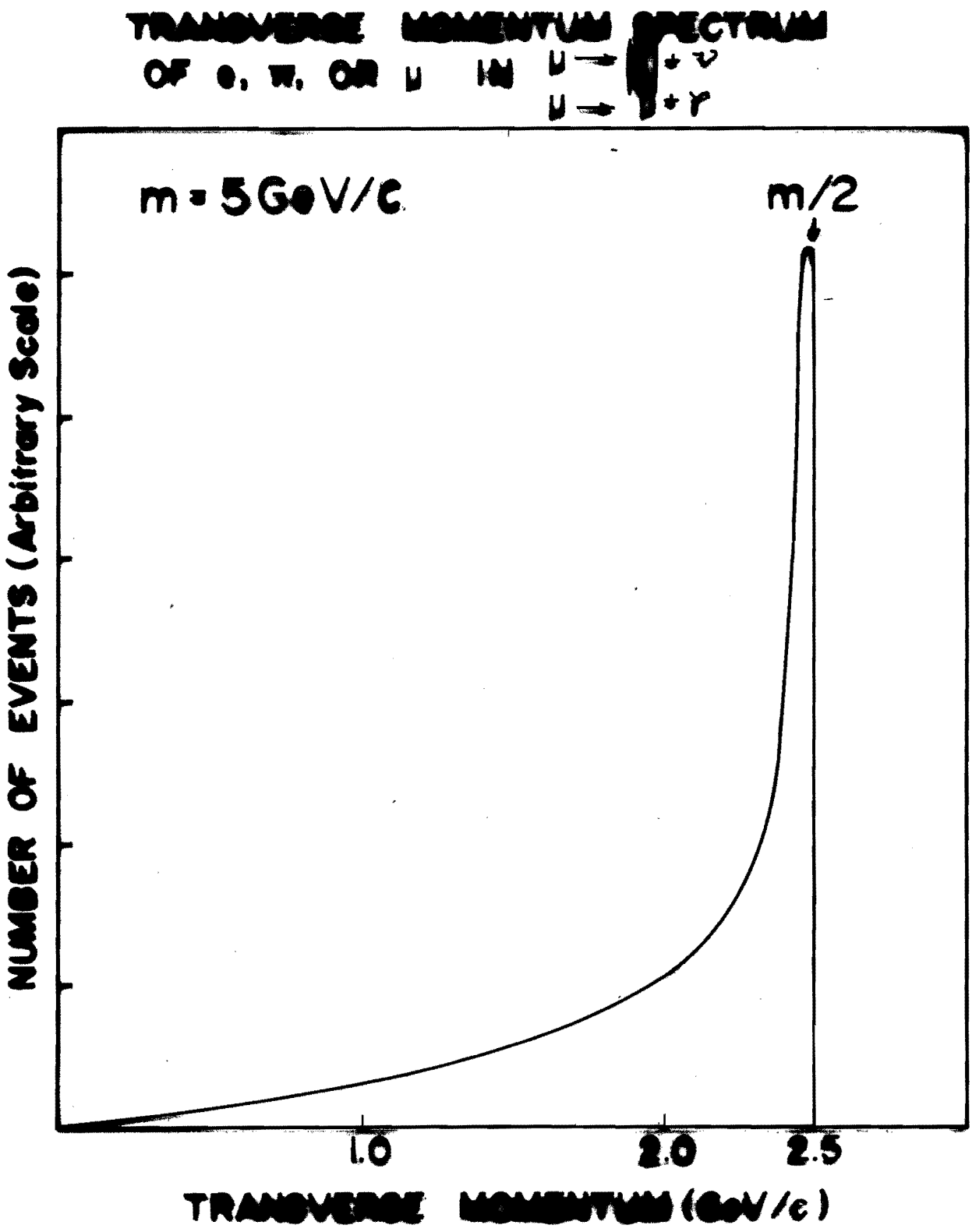
m = 5 GeV/c
m/2
NUMBER OF EVENTS (Arbitrary Scale)
1.0
2.0
2.5
TRANSVERSE MOMENTUM (GeV/c)

A charged-lepton particle pair (M^+,M^-) can be created via the deep inelastic reaction

$$\mu+Z \rightarrow M^+ + M^- + \mu + Z \tag{24}$$

resulting a three-muon final state. Among the decay channels detected in this experiment are

$$M^{\pm} \rightarrow \begin{cases} \pi^{\pm} + m\nu & m = 1,3,. \\ \mu^{\pm} + n\nu & n = 2,4,.. \end{cases} \tag{25}$$

To observe the $M^{\pm}$ the transverse-momentum spectrum of the decaying e, μ or π pairs, or combinations thereof are measured. In Fig. 14 the transverse-momentum spectrum of the e, μ and π in the laboratory for the decay of a m_M = 5-GeV particle via single-neutrino or single γ emission (or any two-body decay) is displayed. The pronounced peak and sharp cutoff at $m_M/2$ of the transverse-momentum spectrum depends upon the mass of the parent particle and is independent of the energy of the incident virtual photon.[17] The width of the peak in the transverse-momentum spectrum will be broadened due to the distribution of finite transverse momenta with which the $M^{\pm}$ are produced. In our experiment this effect does not make a significant contribution to the width.

The transverse-momentum spectrum of the e or μ in the three-body leptonic decay

$$M \rightarrow \binom{\mu}{e} + \bar{\nu} + \nu \tag{26}$$

also exhibits a sharp cutoff at $\frac{m}{2}$, if the matrix element for this decay follows the conventional V - A theory. The cutoff of the transverse-momentum spectrum of the decay particle is the same for both the two-body and three-body decay modes, although the actual distributions are different.

4) Muon Tridents

$$\mu^+ + Z \rightarrow \mu^+ + \mu^- + \mu^+ + Z \qquad (27)$$

The technique used here is to rely on the absence of sharp cutoff in $P_\perp$ of muons and to detect μ^- momentum spectrum.

C. Event Rate Considerations

As will be discussed in sufficient detail later, the cross sections of the processes we propose range from $\sigma \gtrsim 10^{-34}$ cm^2 (deep inelastic scattering) to $\sigma \tilde{-} 10^{-37}$ cm^2 ($M^\pm$ production). It is quite clear that a massive target (~ 16 meters equivalent of iron, see Table I) and a large integrated flux are necessary. Table V shows the parameters of this experiment.

Table VII.

flux, f	10^{12} -10^{13} muons
target thickness in number nucleons, N	1.32×10^{26}
fN	1.3×10^{38} - 1.3×10^{39}

A measurable cross section can be estimated on a crude basis as follows. We assume a detection efficiency of ½ and branching ratio of ~ ½ on the average. Given that 100 events are necessary for a credible search, the minimum cross section for this experiment we have,

$$\sigma_{min} = \frac{100}{1.3 \times 10^{38} \ (\frac{1}{4})(\frac{1}{2})} = 6.2 \times 10^{-36} \text{ cm}^2 \text{ for } f = 10^{12} \text{ muons}$$

and (28)

$$\sigma_{min} = 6.2 \times 10^{-37} \text{ cm}^2 \text{ for } f = 10^{13} \text{ muons}$$

D. Triggering

Three primary event selection or trigger arrangements are permitted by the experimental apparatus. (i) A muon interaction in the iron deflection magnet target is signified by charged particles emerging from that target and entering the calorimeter; one of the particles, presumably a muon, is required to penetrate $59\ell_c$ of material; the total energy of the remaining particles is required to be greater than (10 - 15) GeV. (ii) A noisy muon interaction in the calorimeter is signified by absence of other charged particles incident on it; by one of the product particles on average traversing $38.7\ell_c$ of material; by the total energy of the remaining particles being greater than (10 - 15) GeV. (iii) A quiet muon interaction in the calorimeter is signified by the absence of incident charged particles; by two or three of the product particles on average traversing $38.7\ell_c$ of material; by the absence of other charged particles with total energy $\gtrsim$ 0.5 GeV. There will be an additional trigger mode for quiet low momentum transfer quasielastic events. The event rates for these processes will be high enough to allow appropriate discrimination levels to be set empirically in the experiment. Furthermore, the construction of the calorimeter makes it possible to explore the effects of varying the cutoff on the muon energy.

The relative compactness of the ionization calorimeter is important in reducing the number of charged pion decays in flight in hadron showers produced in it. On average the pions will undergo a nuclear interaction in traversing $1.5\ell_c$ of material, i.e., about 0.5 m of length in the calorimeter. For example, the mean

decay length of a 4 GeV pion is 225 m and thus less than about 1 in 700 such pions will decay to give a muon of energy greater than 3 GeV before interaction. The fraction of pions that decays decreases linearly with increasing pion momentum.

Needless to say, scintillation counter banks and proportional chambers will be employed to select one or multiple number of muons at large transverse momentum for further background suppression. A detailed Monte-Carlo study will be submitted as an addendum to this proposal.

V. COST ESTIMATE

Consistent with past practices, we list in sufficient detail the cost estimate for principal items to be used in the experiment. We note that the existence of E-26 spectrometer reduces the cost by 2/3 the entire amount. To construct and assemble the MIC, we suggest a cost of $175,000 over two years.

A. Muon Interaction Calorimeter

No.	Item	Particulars	Qty	Unit	Rate	Approximate Cost
1.	Lead Plates	Number = 1600 Av. Size = 40"x40" Thickness = 1/8"	65	tons	200.00	14,000.00
2.	Liquid Scintillator	Volume = 470 ft^3	14.5	tons	1000.00	14,500.00
3.	Aluminum cladding (alloy 1100-0)	Thickness = .04" (on both sides of lead plates in item 1)	6.0	tons	800.00	4,800.00
4.	Lucite for container for liquid scintillators	4 mm thick lucite	750	sq.ft.	2.00	1,500.00
5.	Labor for container size 3.5 x 3.5 x 42 ft			Lumpsum		5,000.00
6.	Labor for calorimeter			Lumpsum		15,000.00
7.	Photomultipliers	EMI 5"	144	units	200.00	28,800.00
8.	Photomultiplier bases		144	units	50.00	7,000.00
9.	Light pipes		144	units	100.00	14,400.00
10.	Electronics and labor for photomultipliers			Lumpsum		10,000.00
11.	Structure to support calorimeter			Lumpsum		10,000.00
12.	Proportional wire chambers		24	units	500.00	12,000.00

B. Iron Deflecting Magnet

1.	Iron costs (2.4 x 2.4 x 12 ft)		17	tons	500.00	8,500.00
2.	Coils			Lumpsum		3,500.00

		Approximate Cost
C. Muon Analyzing Spectrometer		
1. Eight solid iron magnets	Exist with Exp. #26	0
2. Spark chambers and readont system	Exist with Exp. #26	0
3. Proportional chambers and readont system	Exist with Exp. #26	0
4. Scintillation counter banks	Exist with Exp. #26	0
	Total	149,000.00
	contingency 15% of above	22,350.00
	Grant Total	171,350.00

VI. SCHEDULE AND TIME TABLE

This experiment can be assembled at the conclusion of Experiment #26. The major equipment required is the muon interaction calorimeter (MIC). It is fortunate that muon beam is well defined in space so that the size of the calorimeter is moderate. We estimate that ½ year would be sufficient for construction and an additional 3 months to be spent on calibration of MIC. Allowing 3 months for final assembly, we estimate that one year from the date of approval the MIC will be ready for experimentation. Allowing one year to complete E-26 from September, 1973, we would like to start setting up the experiment in January, 1975.

The experiment will require about 2000 hours of data, taking time for 5×10^{12} protons incident on the Neutrino Laboratory target.

Scientific personnel named in this proposal are all postdoctoral level staff associated with the universities cited. We expect to add several graduate students as the preparation of the experiment is underway.

VII. REFERENCES

1. F. E. Low, Phys. Rev. Letter 14 238 (1965), A. O. Barut, P. Cordero, and Ghiardi, Phys. Rev. 182, 1844 (1969).

2. J. D. Bjorken and C. H. Lewellyn-Smith, Phys. Rev. 7 887 (1973).

3. M. Nauenberg, International Symposium on Electron and Photon Interactions at High Energies, Ithaca, N.Y. (1971).

4. K. W. Chen, 1969 NAL Summer Study.

5. C. Lichtenstein, W. W. Ash, K. Berkelman, D. L. Hartill, R. M. Littauer and R. H. Siemann, Phys. Rev. ID 825 (1970).

6. S. Brodsky and S. C. C. Ting, Phys. Rev. 145 1018 (1966); J. D. Bjorken and M. C. Chen, Ibid. 154 1335 (1967); M. J. Tannenbaum, ibid. 167 1308 (1968).,and 1970 NAL summer study.

7. S. Weinberg, Phys. Rev. Letter 19 1264 (1967), 27 1688 (1971, Phys. Rev. D5 1412 (1972), and D5 1962 (1972, and Ref. (2).

8. K. J. Kim and Y. S. Tsai, SLAC-PUB-1105 (1972).

9. K. W. Chen and L. N. Hand, "High Momentum Transfer Inelastic Muon Scattering and Test of Scale Invariance at NAL", NAL Proposal No. 26 (1970).

10. H. Fearing, M. Pratap and J. Smith, Phys. Rev. 5 158 (1973).

11. T. D. Lee and G. C. Wick, Phys. Rev. D2 1033 (1970).

12. R. Linsker, Phys. Rev. 5 1709 (1972).

13. F. Brasse, Private Communication.

14. K. Runge, Private Communication.

15. J. Ranft, ParticlesAccelerator, 3 129 (1972)

16. Van Ginnekan, NAL FN.250, NAL Technical Report

17. W. Lee et. al., NAL Proposal No. 87., "Proposal to Search for Heavy Leptons and Intermediate Bosons from Photon-Nuclei collisions.

APPENDIX I

Calculation of Lepton Pair Muoproduction

Exact theoretical calculations of muon induced process are in general exceedingly lengthy and tedious. It is, however, possible to write down simple expressions for muoproduction which are related to corresponding photoproduction processes.

In the limit of zero momentum transfer, the following expressions are exact

$$\lim_{q^2 \to 0} \sigma_T (\nu, q^2) = \sigma_\gamma (k) \qquad \text{A (1)}$$

$$\lim_{q^2 \to 0} \sigma_L (\nu, q^2) = 0 \qquad \text{A (2)}$$

where σ_T = cross section for transversely polarized virtual photon

σ_L = cross section for longitudinally polarized virtual photon

ν = energy transfer from muons

q^2 = 4-momentum transfer

$$= 4\, E(E-\nu)\, \sin^2 \frac{\theta}{2} + \frac{m_\mu^2\, \nu^2}{E(E-\nu)}$$

σ_T and σ_L are related to the structure functions W_1 and W_2

$$W_1 = \frac{1}{4\pi\alpha^2} \left(\frac{q^2}{\nu^2+q^2}\right)^{1/2} \left[\sigma_L (\nu, q^2) + \sigma_T (\nu, q^2)\right] \qquad \text{A (3)}$$

$$W_2 = \frac{1}{4\pi\alpha^2} \left(\frac{q^2}{\nu^2+q^2}\right)^{1/2} \left(1 - \frac{2m_\mu^2}{q^2}\right) \frac{\nu^2+q^2}{q^2}\, \sigma_T (\nu, q^2) \qquad \text{A (4)}$$

The pair production by real photons for a lepton with mass m_e,

near the forward angle ($\theta << 1$) and for relationship ℓ's ($E^+ >> m_\ell$ and $E^- = (k - E^+) >> m_\ell$) is given by

$$\frac{d\sigma}{dk} = \sigma_\gamma(k) = \frac{4}{137} r_o^2 \frac{m_\mu^2}{m_\ell^2} \frac{1}{k} \left[1 - \frac{4}{3} \frac{E(k-E)}{k^2}\right]\left[\ell n \frac{2E(k-E)}{km_\ell} - \frac{1}{2}\right]$$

A (5)

near the forward angle ($\theta << 1$) and for relationship ℓ's ($E^+ >> m_\ell$ and $E^- = (k - E^+) >> m_\ell$) is given by

$$\frac{d\sigma}{dk} = \sigma_\gamma(k) = \frac{4}{137} r_o^2 \frac{m_\mu^2}{m_\ell^2} \frac{1}{k} \left[1 - \frac{4}{3} \frac{E(k-E)}{k^2}\right]\left[\ell n \frac{2E(k-E)}{km_\ell} - \frac{1}{2}\right] \qquad A\ (5)$$

where $r_o = 2.818 \times 10^{-13}$ cm

k = photon energy

E = muon energy

$\sigma_\gamma(k)$ depends on $\frac{1}{m_\ell^2}$. This is related to the minimum value of the lepton propagator which is related to m_ℓ^2.

Since the minimum value of the lepton propagator in a virtual photon induced process is $q^2 + m_\ell^2$, we could assume that

$$\sigma_T(\nu, q^2) \sim \sigma_\gamma(k) \frac{m_\ell^2}{m_\ell^2+q^2} \qquad A\ (6)$$

A further simplification can be obtained by approximating

$$\sigma_L(\nu, q^2) << \sigma_T(\nu, q^2) \qquad A\ (7)$$

The pair production cross section by muons can now be written as

$$\frac{d^2\sigma}{dEd\Omega} = \frac{2}{137} r_o^2 \frac{m_\mu^2}{(m_\ell^2+q^2)} \frac{E^2\gamma^2}{\nu^2} \left[\frac{16\ell(1-y)}{(1+\ell)^4} - \frac{(2-y)^2}{(1+\ell)^2} - \frac{2(1-y)+y^2}{(1+\ell^2)} - \right.$$

$$\left. - \frac{4\ell(1-y)}{(1+\ell)^4} \ell n \frac{q^2\ min}{m_\ell^2(1+\ell)^2}\right] \qquad A\ (8)$$

where E = energy of lepton production

ν = energy of virtual photon

$$\gamma = \frac{E}{m_\ell}$$

$$\ell = \gamma^2\theta^2$$

$$y = \frac{\nu}{E}$$

$$q^2_{min} = \frac{\nu m_\ell^2 (1+\ell)}{2E(\nu - E)}$$

If $\nu >> \gamma^2\theta^2$ we can integrate over Ω yielding

$$\frac{d\sigma}{d\nu} = \frac{X(\nu)}{\nu}\ \sigma_\gamma(\nu)$$

where
$$X(\nu) = \frac{\alpha}{\pi}\left\{\left[1-\frac{\nu}{E}\ \frac{\nu^2}{E^2}\ \left(\frac{1}{2}+\frac{m_\mu^2}{m_\ell}\right)\right] \ell n \left[1+\frac{m_\ell^2}{m_\mu}\ \frac{E}{\nu}\left(\frac{E}{\nu}-1\right)\right] - \left(1-\frac{\nu}{E}\right)\right\} \quad A\ (9)$$

$X(\nu)$ is the virtual radiator. Since $\sigma_\gamma(\nu)$ is particularly simple (Fig. 7); the expression $\frac{d\sigma}{d\nu}$ can easily be integrated over to yield σ (total).

A (9) can be further simplified

$$X(\nu) = \frac{\alpha}{\pi}\ \left(1-\frac{\nu}{E}+\frac{\nu^2}{\alpha E^2}\right)\ \ell n\left[1+\frac{\Lambda^2}{m_1^2}\ \frac{E}{\nu}\ \left(\frac{E}{\nu}-1\right)\right] \qquad A(10)$$

where $\Lambda^2 = m_\ell^2$

Approximating the energy dependence of logarithm term by a constant value (good approximation for $m_\ell >> m_{electron}$)

$$X(\nu) = \frac{\alpha}{\pi}\ \left(1-\frac{\nu}{E}+\frac{\nu^2}{2E^2}\right)\ \ell n\ \left(1+\frac{2m_\ell^2}{m_\mu^2}\right) \qquad A(11)$$

APPENDIX II

Pulse Height Digitizing

The Lecroy model 2248 Octal ADC is well suited for our needs since it has the required input characteristics and it is CAMAC readable. It's cost is $1950 or $244 per channel. A less expensive method is described below. It consists of an amplitude-to-time converter (ATC) which would interface the analog pulse heights to the time digitizer system already in operation.

The basic idea behind ATC method is to have a module, produce a pulse with a time delay proportional to the pulse height at the input. The A/D conversion is accomplished by recording the time of this pulse with a time digitizer (T.D.) module. A fast pulse A/D usually has 8 bits of precision. The T.D. modules have 14 bits precision and each input can accept up to 8 inputs. Thus multiple ATC's could feed one T.D. input so long as each ATC pulse followed the preceding one by a delay time at least as long as the time to digitize a full scale pulse height (i.e. 8 bits). Each ATC has a capacitor charged to the input pulse height with a linear slow discharge circuit which starts discharging it at a time of a transition of but 9 of the T.D. master scaler. Thus eight ATC's are combined in one module with their delayed pulses ordered in time and recorded by the T.D. module.

Figure A1 shows the time ordering of the system. Note that when the delay times (bits 1-8) are recorded by the T.D., it also records bits 9-14 which serve as identification. Figure A2 shows the physical layout of the ATC module. It must be located

in the same CAMAC crate as the T.D. system. Figure A3 shows a block diagram of the ATC circuit.

The estimated cost of an ATC module is $500. The cost of a T.D. module is $300. Thus the total cost would be $800 for 8 pulse height inputs with 3 inputs to the T.D. either unused or used for other systems, i.e. a cost of $100/channel. If four ATC modules were used with one T.D. module, one would have a 32-channel pulse height system for $2300 or $72/channel.

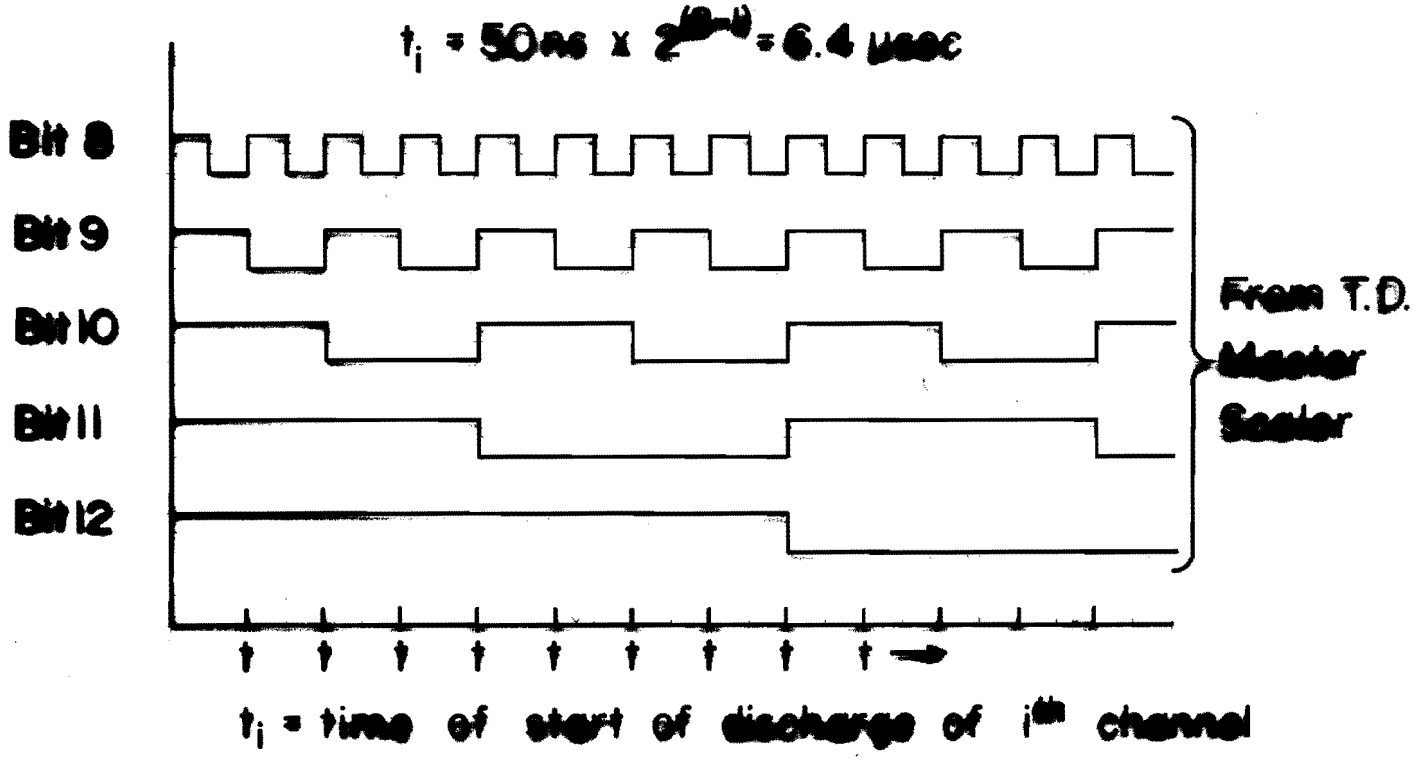

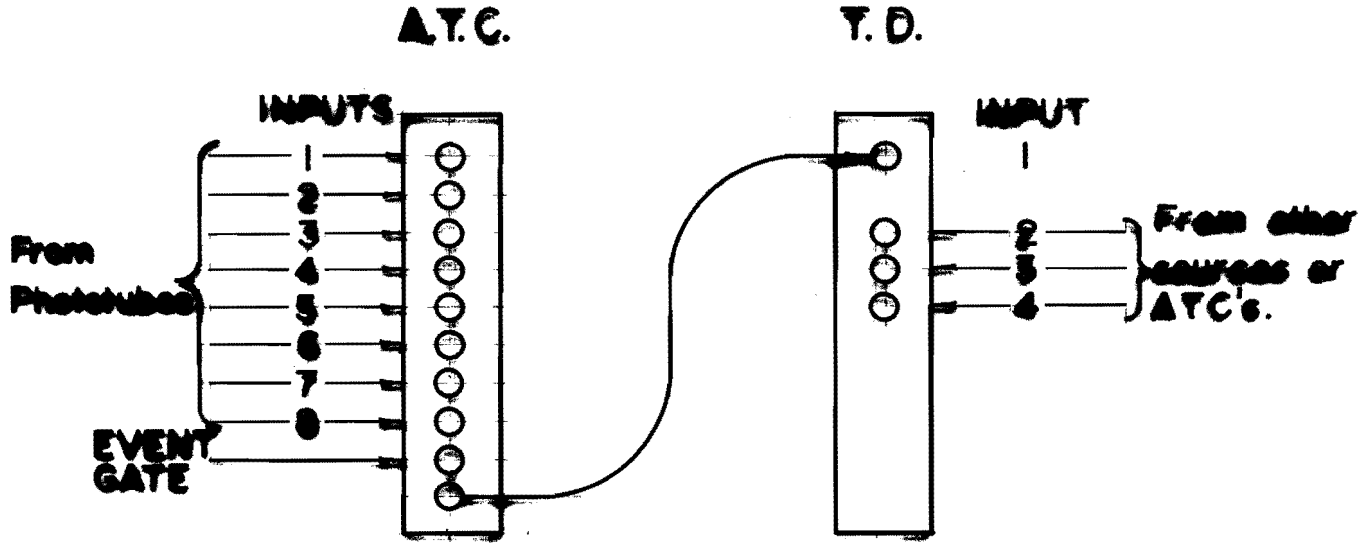

SCHEMATIC OF PULSE CIRCUITS

FIGURE A1

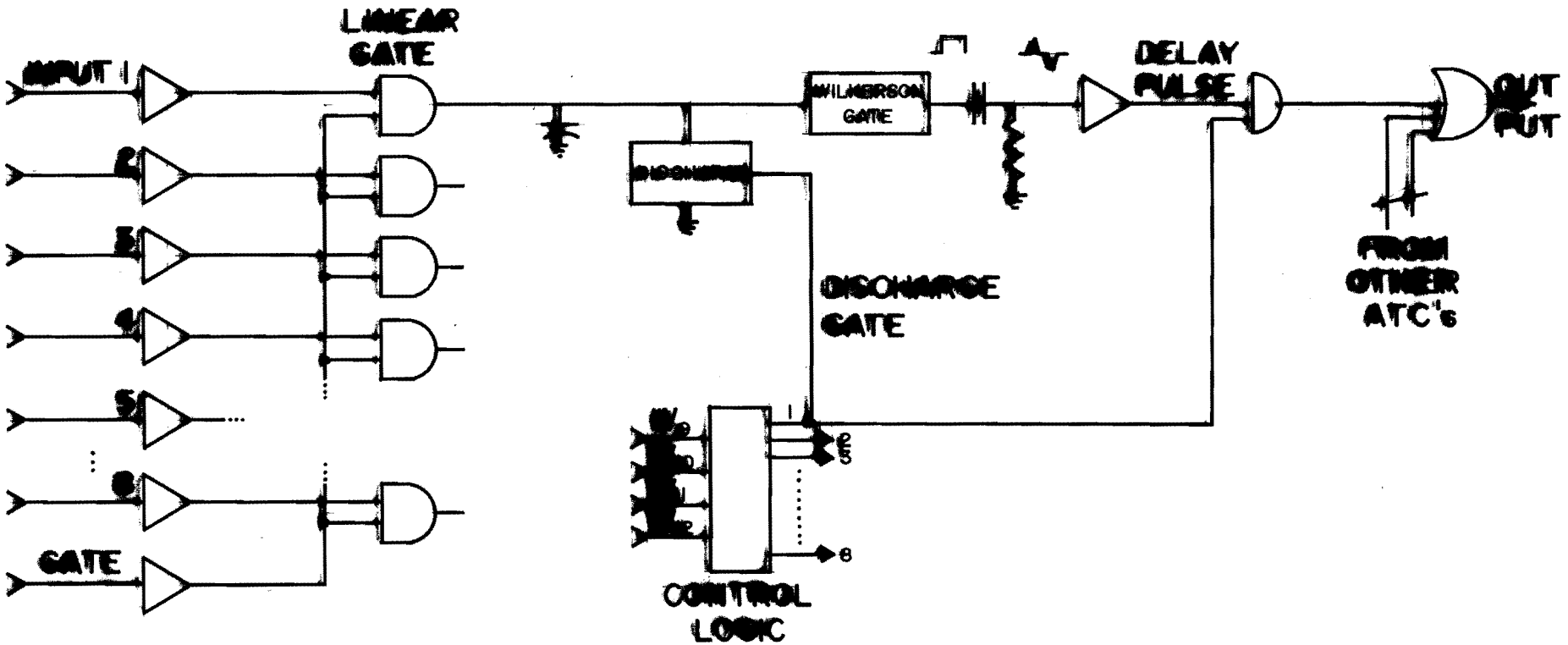

SCHEMATIC OF PULSE CIRCUITS

FIGURE A2

APPENDIX III

Summary of Parameters

I. Iron Deflection Magnet (dimensions)

Length	12.0 ft
Section	2.4 ft x 2.4 ft
Volume	69.1 ft^3
Weight	16.8 tons

II. Fine-Grained Calorimeter

A. Principal Parameters

1. Total Sensitive Parameters

a. Lead plates	70 tons
b. Liquid Scintillator	470 ft^3
c. Aluminum foil (strengthening plates)	6.0 tons
d. Lucite reflecting plates	750 sq ft

2. Thickness

a. Whole sensitive volume	90.52 lb/in^2
b. Single lead plate	0.0512 lb/in^2
c. Single scintillator	0.0072 lb/in^2

3. Energy loss for a relativistic muon

a. To traverse the whole detector	6080.0 Mev
b. To traverse a single lead plate	3.84 Mev
c. In the liquid scintillator for the whole detector	629.5 Mev

4. Nuclear collision lengths

   a. To traverse the whole detector — 59.0

   b. To traverse a single lead plate

5. Radiation lengths (for muon)

   a. To traverse the whole detector — 0.031 r.ℓ.

   b. To traverse MIC — 0.019 r.ℓ.

6. Sensitive volume including Proportional Wire Chambers

   a. Length — 42 ft.

   b. Height — 19, 38, 48, inches

   c. Width — 15, 30, 38, inches

7. No. of Proportional Wire Chambers — 24

8. No. of groups of Lead Scintillator Counters — 23

9. No. of units in each group of Lead Scintillator Counters — 1

10. Lead Scintillator Unit, dimensions and weights

   a. Depth in beam directions — 21 inches

   b. Height — 15, 38, 48 inches

   c. Length — 19, 38, 48 inches

   d. Total weight — 1.525 tons

11. Energy resolutions

   a. For hadronic cascade $E_h \sim 20$ GeV — $\leq 10\%$ (sd)

   b. Energy loss for relativistic muons traversing one lead scintillator unit — $\leq 10\%$ (+Landau tail)

c. Minimum detected (hadron) energy loss in addition to one relativistic muon in liquid scintillator — ~2.50 MeV

Total number of Photomultipliers — 144

Total number of Independent Pulse Height Chambers — 144

B. Lead Scintillator Unit

1. Sensitive Volume

a. Depth in beam direction — 21 in.

b. Height — 15 in, 30 in, 38 in.

c. Width — 19 in, 38 in, 48 in.

2. Lead Plates

a. Number — 63

b. Sizes — 15x19; 30x38; 38x48in.

c. Thickness — 0.125 in.

d. Strengthening — Aluminum foil glued to each side

3. Liquid Scintillator Slabs

a. Number — 63

b. Sizes — 15x19; 30x38; 38x48in.

c. Thickness — 0.20 in.

d. Material of container — Lucite

e. Volume liquid scintillator — 12,000 in^3

f. Type of scintillator — Shell sol A+P- TERPHENIL + POPOP

4. Photomultipliers

a.	Number	3; 6; 9
b.	Type	EMI, 5"
c.	Number of slabs viewed by each photomultiplier	21; 10; 7

APPENDIX IV

EXPERIMENT #26 SPECTROMETER

1.	Number of disks		8
	Disk dimensions	inner hole	15" diameter
		outer diameter	71.5" nominal
		thickness	32" nominal
2.	Ampere turns/disk		22,500
	Amperes		50 Amps.
3.	Turns/disk		480
4.	Wire type for coil		#8 stranded copper
5.	Resistance of coil/disk		3.01 ohm (20°C) 3.37 ohm (50°C) 3.67 ohm (75°C)
6.	Voltage across disk coil		150.7 volts (20°C) 168.5 volts (50°C) 183.3 volts (75°C)
7.	Power required/disk, assuming 175v.		8.75KW
	Total power required, 8 units		70KW
8.	H in oersteds	outer radius	45
		inner radius	215
	B in kilogauss	outer	16.0
		inner	18.7
	% change	inner-outer	15.5%

MICHIGAN STATE UNIVERSITY
DRAWING NO. 201
MAGNET CONFIGURATION
EXP. NO. 26 NAL

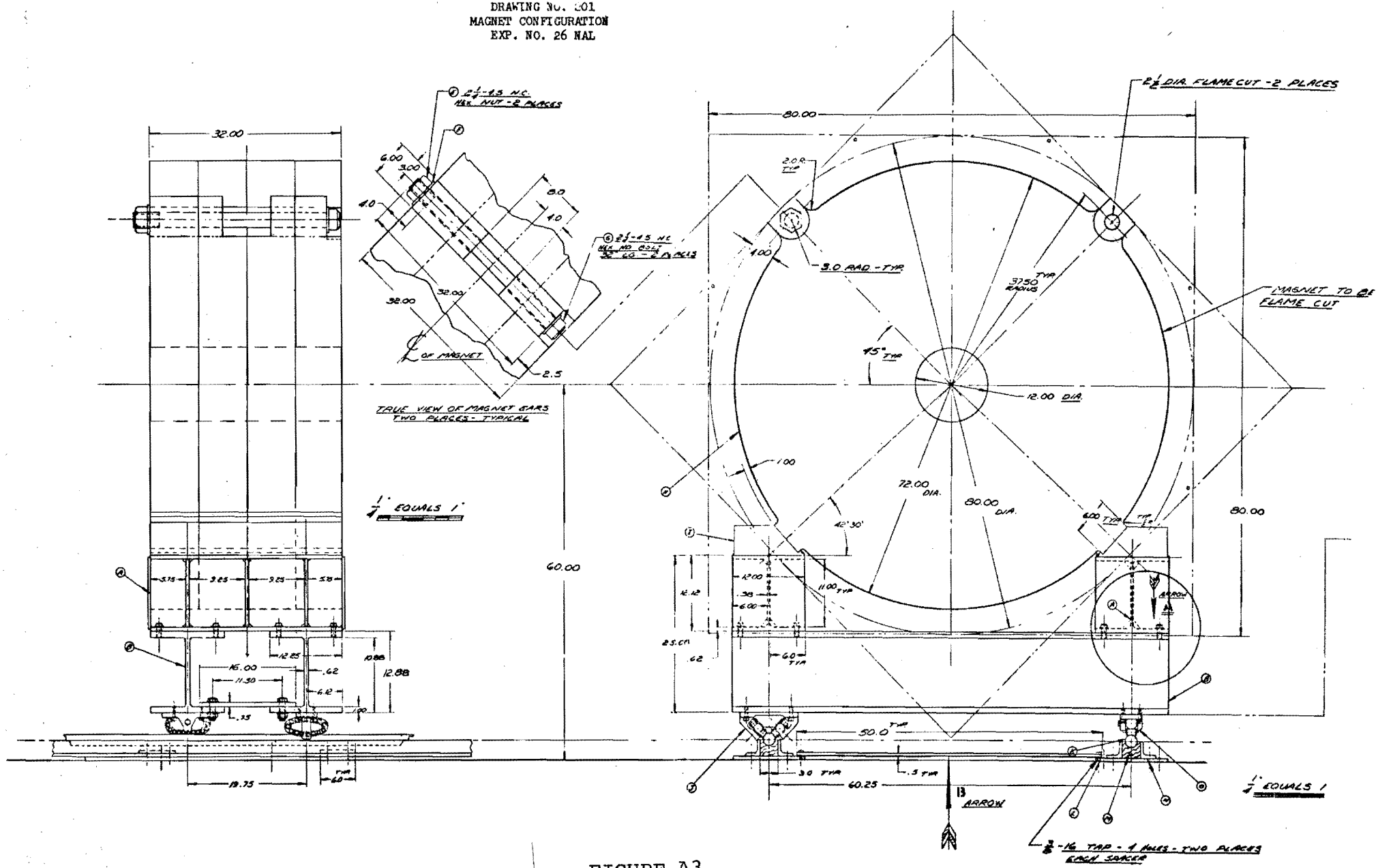

FIGURE A3

ZMIN: 0.03 DMIN: 7.06

$Q^2 = 50 \frac{GeV^2}{c^2}$

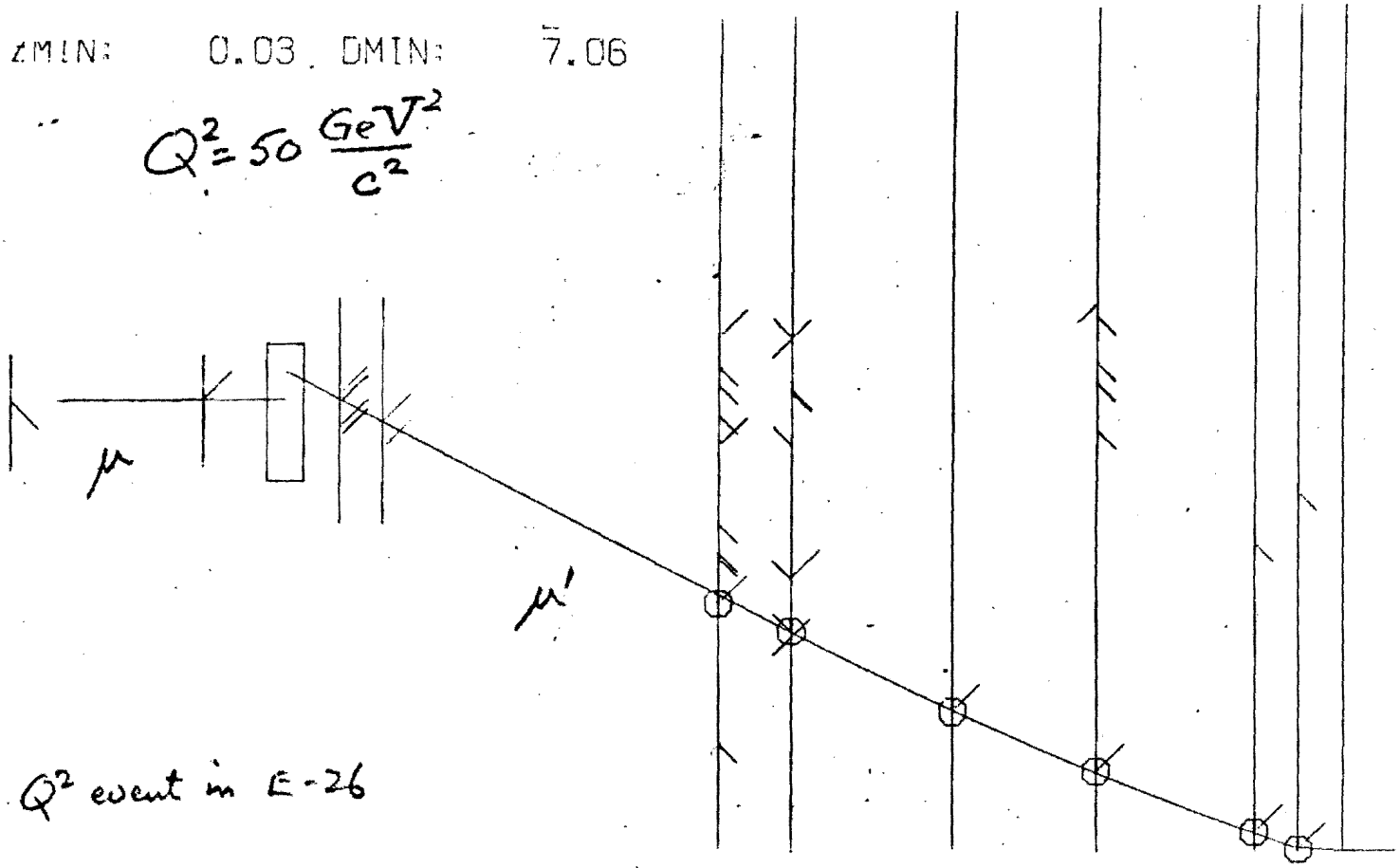

high Q^2 event in E-26

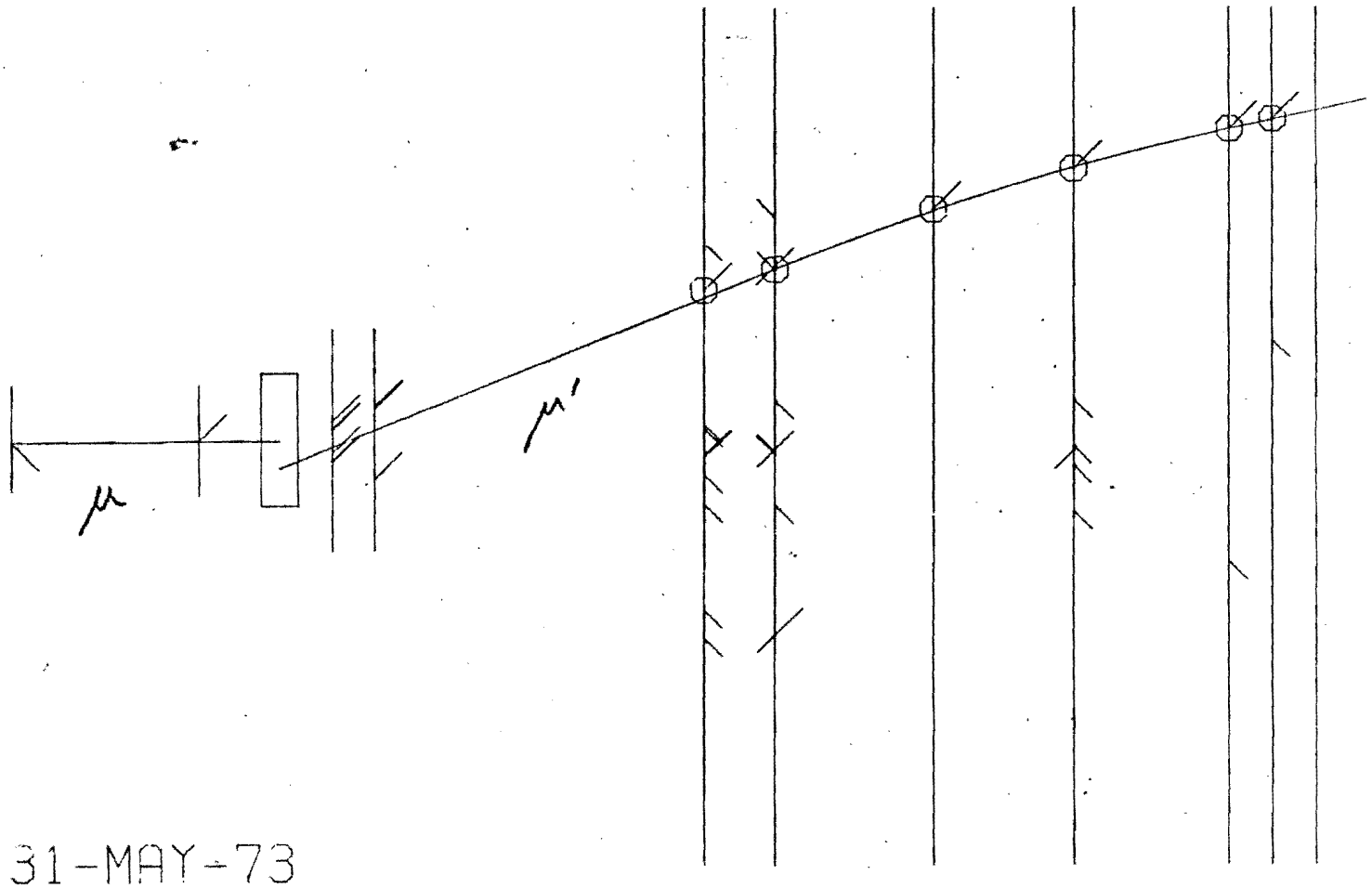

31-MAY-73

HOR. VIEW RUN: 100 EV: 10
X2-AS 0.00 0.01 0.12 0.13
OVRFL 00000000 #TRK 2
ZMIN: 0.03 DMIN: 7.06

$Q^2 = 50 \frac{GeV^2}{c^2}$

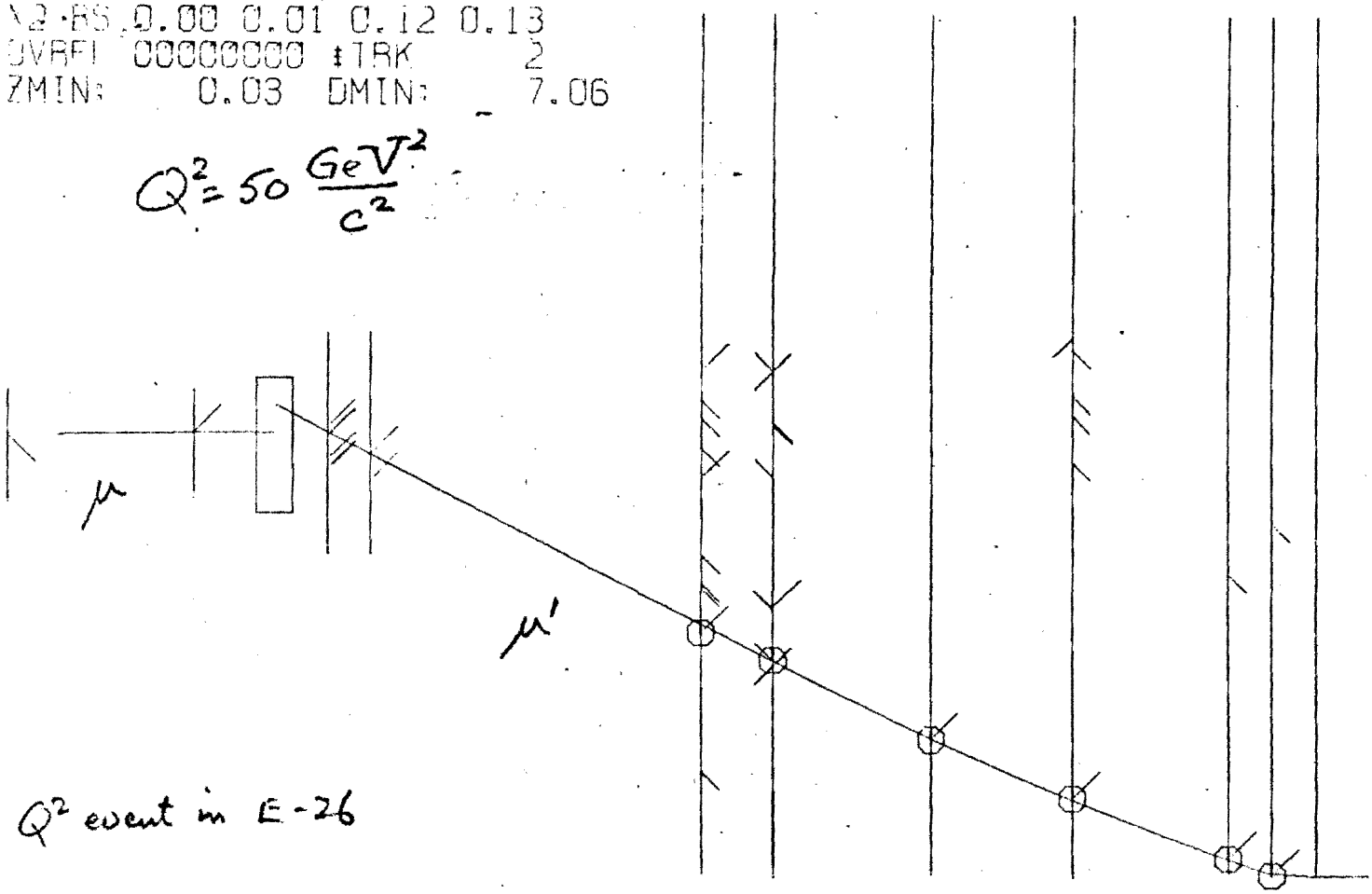

High Q^2 event in E-26

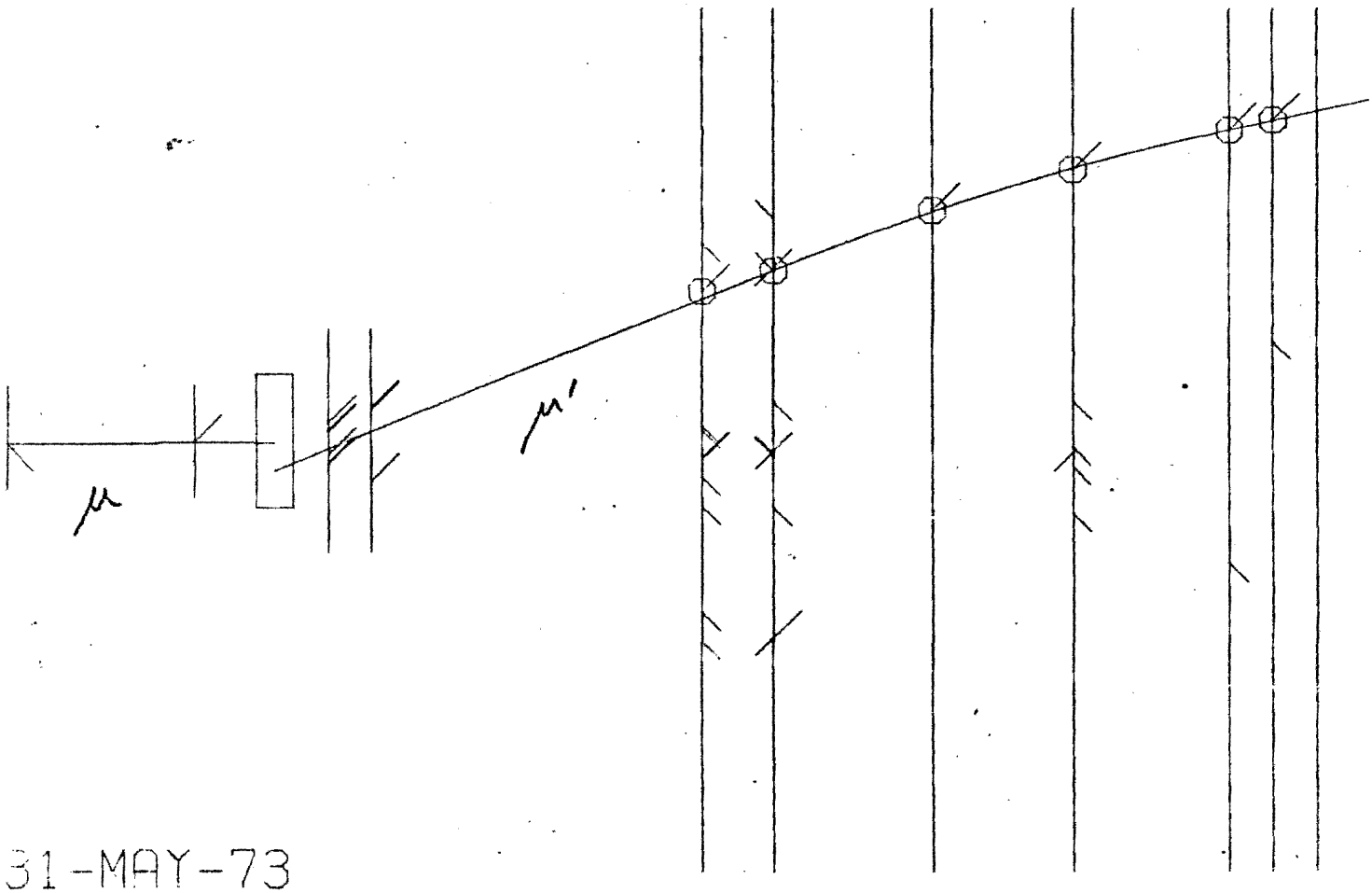

31-MAY-73

SECONDARY FIT, CHISQUARED(R)/DEGREE OF FREEDOM

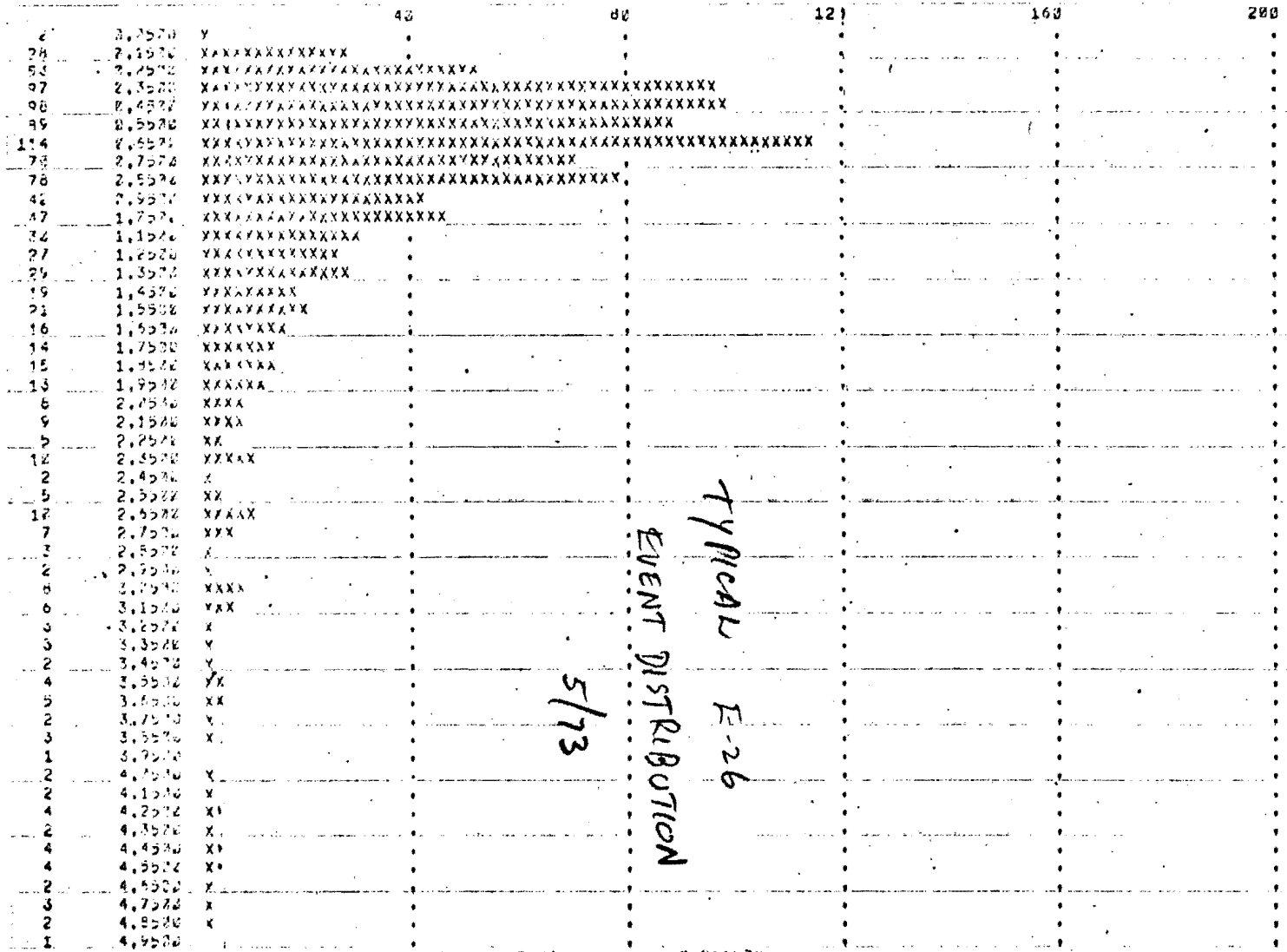

1020 EVENTS IN PLOT, MEAN= 1.060982 AND SIGMA= 0.911978

TYPICAL E-26 EVENT DISTRIBUTION 5/73

QUEUE SWITCHES: /PRINT:ARROW /FILE:FORT /COPIES:1 /SPACING:1 /LIMIT:62

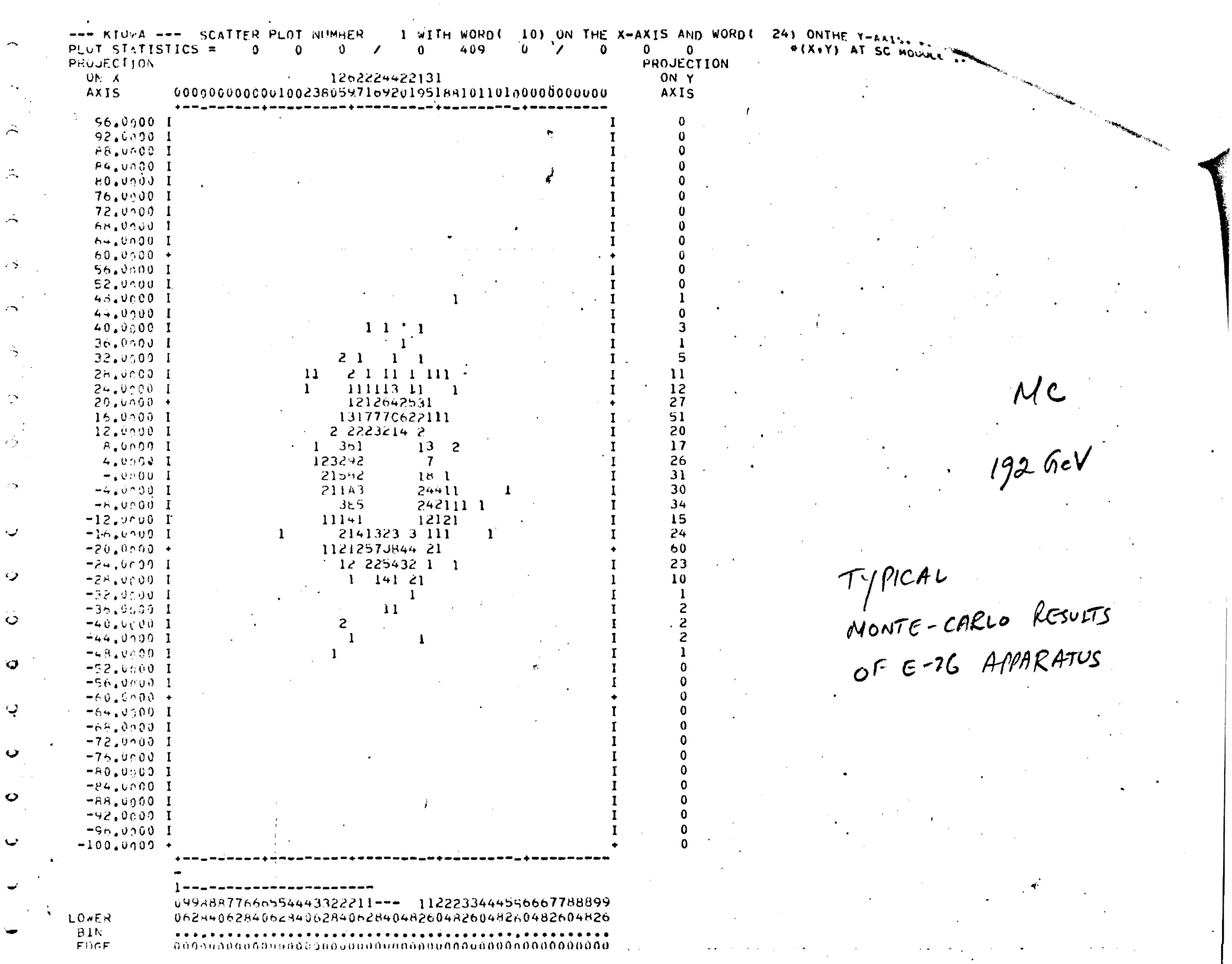
--- KIOWA --- SCATTER PLOT NUMBER 1 WITH WORD(10) ON THE X-AXIS AND WORD(24) ONTHE Y-AXIS
PLOT STATISTICS = 0 0 0 / 0 409 0 / 0 0 0
PROJECTION ON X AXIS
PROJECTION ON Y AXIS
LOWER BIN EDGE
MC
192 GeV
TYPICAL MONTE-CARLO RESULTS OF E-26 APPARATUS

MUON AREA

EXPERIMENT 98 APPARATUS

THIS PROPOSAL

IRON DEFLECTION MAGNET

MUON INTERACTION CALORIMETER

EXPERIMENT 26 SPECTROMETER

SC 1 SC 2 SC 3 SC 4 SC 5 SC 6 SC 7 SC 8

12'-0" 14'-0" 14'-0" 14'-0" 90'-0" TOTAL

0.35 36'-0"

2 BAYS AT 30'-0" = 60'-0"

7 BAYS AT 20'-0" = 140'-0"

200'-0" TOTAL

19'-0"

80'-0" 40'-0" 14'-0"

A

0 2 0 4 8 12 FEET

MICHIGAN STATE UNIVERSITY
COUNTER SPARK CHAMBER LABORATORY

PROPOSED EXPERIMENTAL AREA

SCALE 1/4"=1'-0" DATE 4-9-73

DRAWN BY B. DAVISON APPROVED BY K.W. CHEN